Electronic Supplementary Material (ESI) for Physical Chemistry Chemical Physics.
This journal is © the Owner Societies 2020

Supplementary Information

The Application of MM/GBSA Method in the Binding Pose Prediction of FGFR Inhibitors

Yu Chen,[a,‡] Yongxiang Zheng, [a,‡] Shengjun Mao,[a] Pedro Fong[b] and Qiantao Wang[a,*]

[a.] Key Laboratory of Drug-Targeting and Drug Delivery System of the Education Ministry, Sichuan Engineering Laboratory for Plant-Sourced Drug and Sichuan Research Center for Drug Precision Industrial Technology, West China School of Pharmacy, Sichuan University, Chengdu 610041, China.

[b.] School of Health Sciences and Sports, Macao Polytechnic Institute, Rua de Luís Gonzaga Gomes, Macao, China

[‡]These authors contributed equally.

*Corresponding author: Qiantao Wang (qwang@scu.edu.cn).

Table of Contents

1. Supplementary Figures

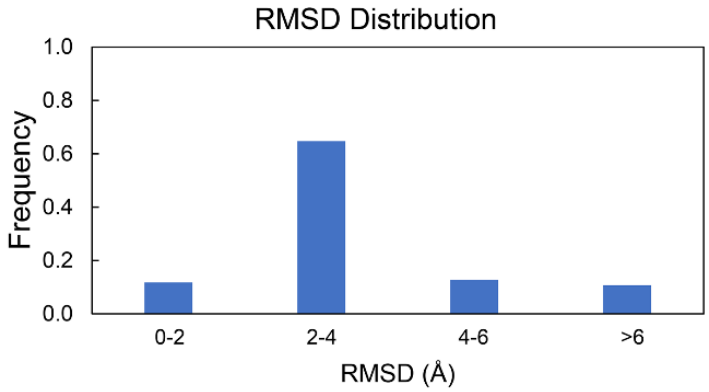

Figure S1. The distribution of RMSD values of poses generated by Autodock Vina. The RMSD was calculated against the top ranked pose of each ligand.

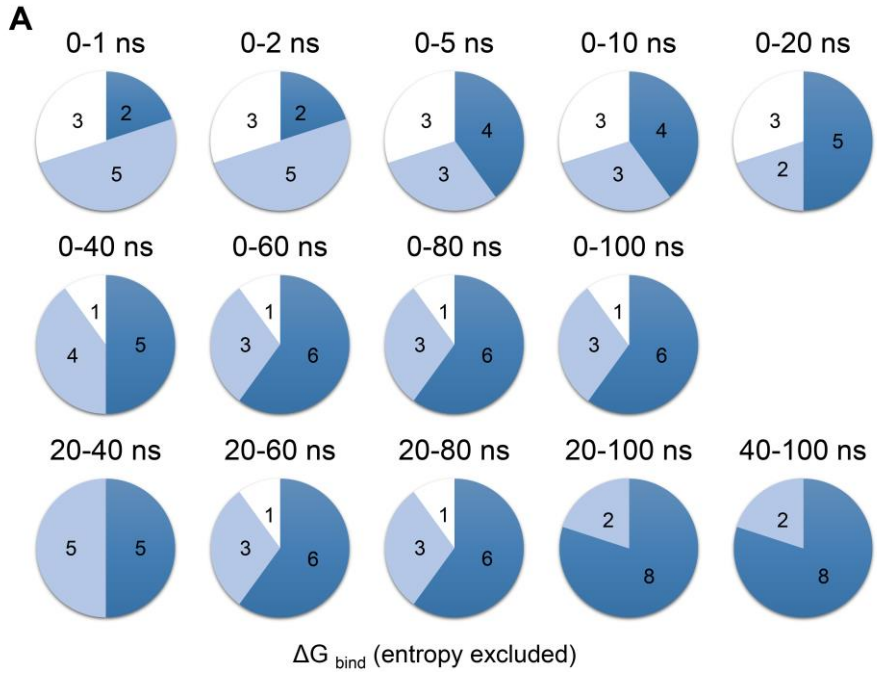

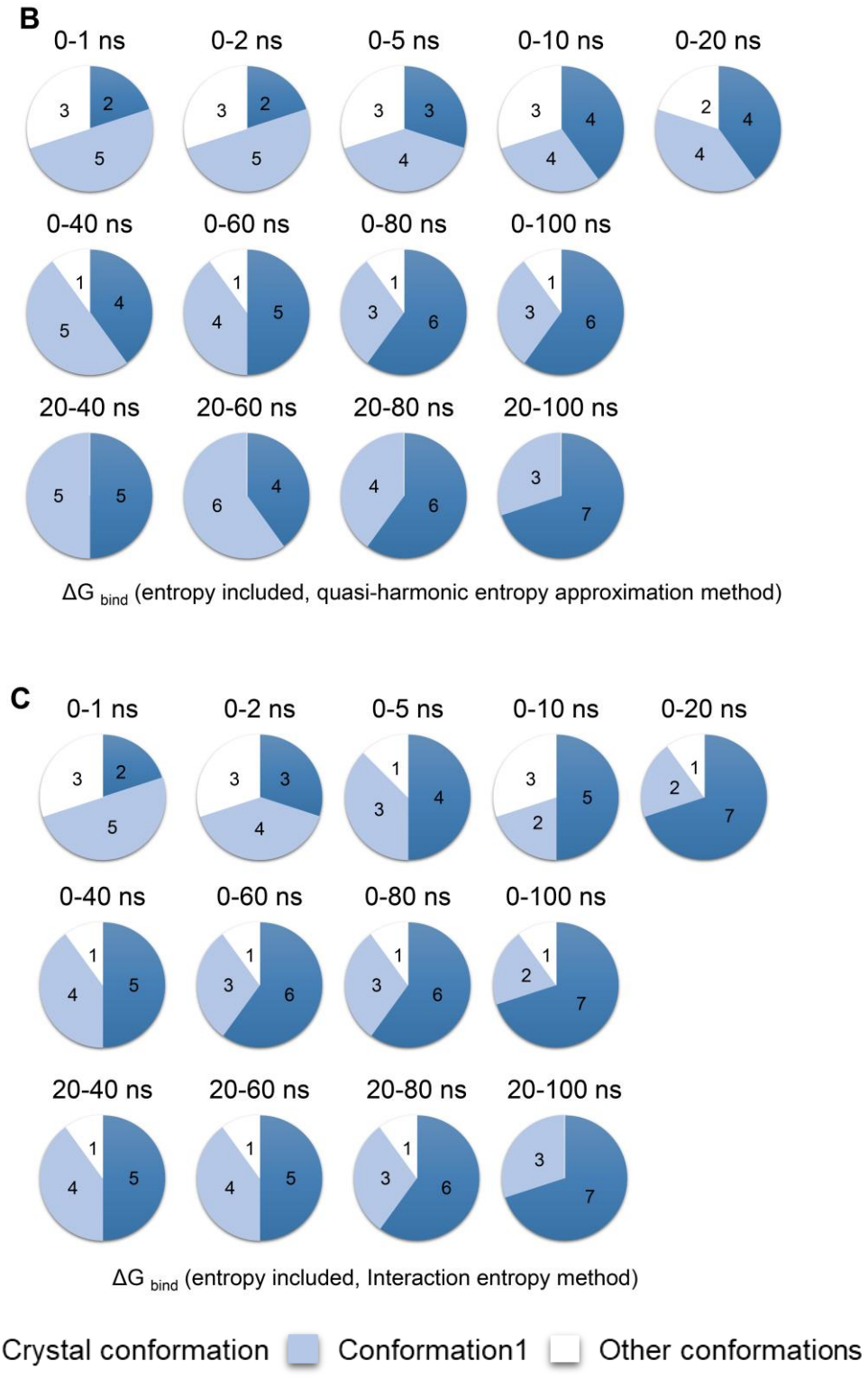

Figure S2. Pie charts show the correct cases that MM/GBSA predicts the crystal conformation being the lowest energy pose in a serial of time periods. MM/GBSA binding energy without entropy (A), with the quasi-harmonic analysis entropy (B) and

with the interaction entropy[1] (C) were separately demonstrated. The area in dark blue corresponds to crystal conformation had the lowest energy, light blue corresponds to that conformation1 (the conformation that was closest to the crystal structure was ranked as conformation 1 using AutoDock Vina) had the lowest energy and white corresponds to that other conformations had the lowest energy.

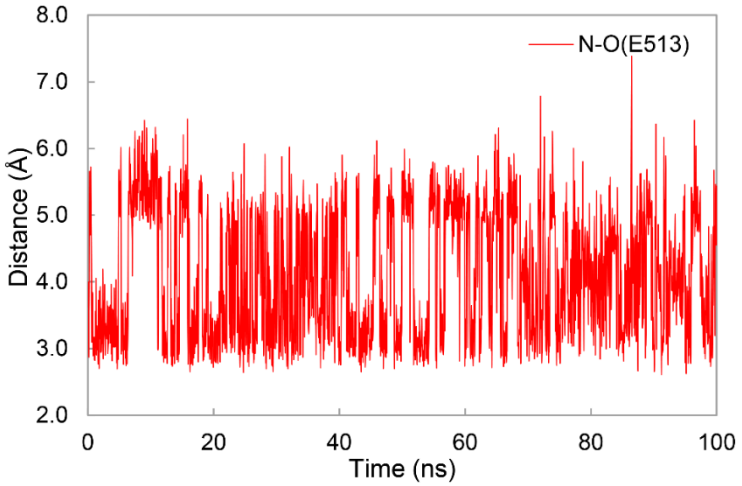

Figure S3. The hydrogen bond (N-O (E513)) between E3810-con2 and FGFR1 was not stable during the 100 ns MD simulation.

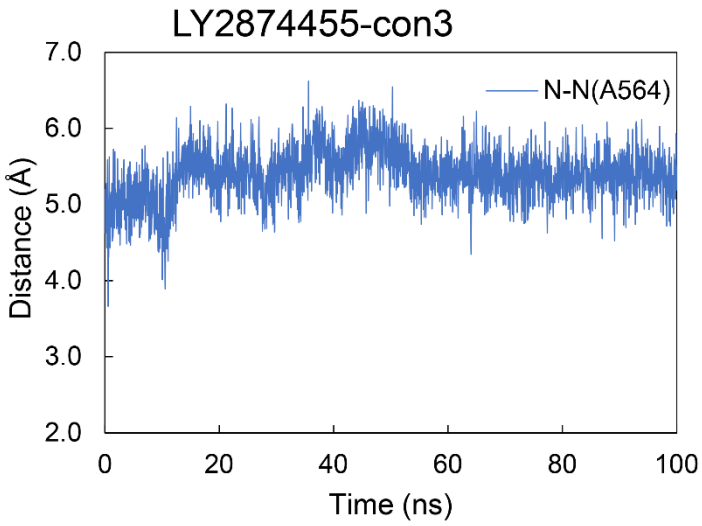

Figure S4. The distance between the indazole ring of LY2874455-con3 and residue A564 in the hinge region of FGFR1 was 5.4 ± 0.3 Å (N-N (A564)) during the 100 ns simulation, indicating there is no hydrogen bond between them.

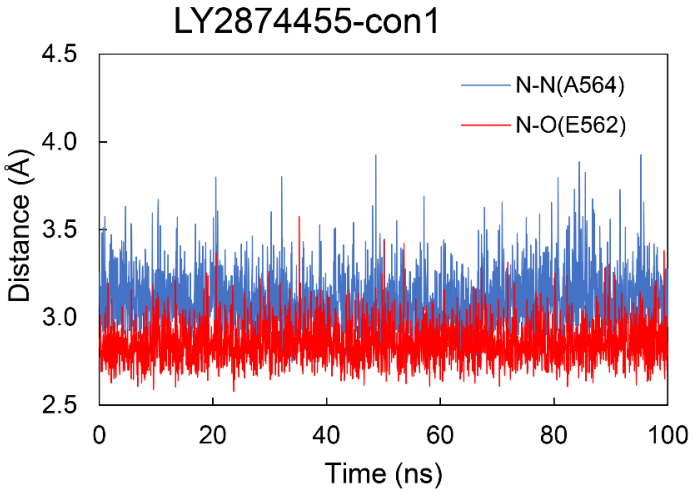

Figure S5. The hydrogen bonds between LY2874455-con1 and FGFR1 remained stable during the 100 ns simulation, given the average hydrogen bond distances of 3.1 ± 0.2 Å for N-N (A564) (in blue) and 2.9 ± 0.1 Å for N-O (E562) (in red). This is in line with the binding free energy predicted by MM/GBSA (Figure 6D).

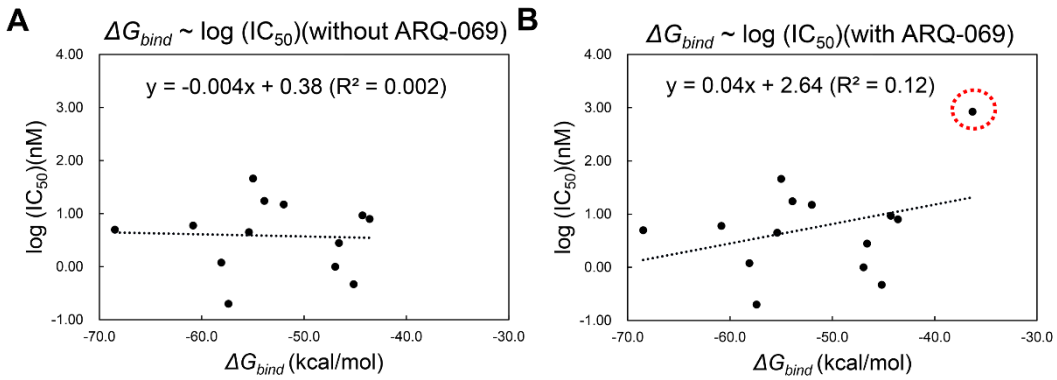

Figure S6. The addition of a ligand with weaker affinity significantly changed the correlation coefficient between the calculation and experiment results for strong binders. This is a simple demonstration that may explain the different performance of MM/GBSA method reported in literature to some extent. The scatter plot of MM/GBSA and experimental results for strong binders, whose IC_{50} vales against FGFR1 ranges from 0.2 to 50 nM, shows a rather low R^2 correlation coefficient (0.002). (B) The scatter plot of MM/GBSA and experimental results for strong binders plus ARQ-069 (the dot in the circle of red dotted lines), a weak binder with IC_{50} value of 840 nM, shows a relative higher R^2 correlation coefficient (0.12). ΔG_{bind} predicted by MM/GBSA was taken from the lowest ΔG_{bind} among all the conformation for each ligand we calculated.

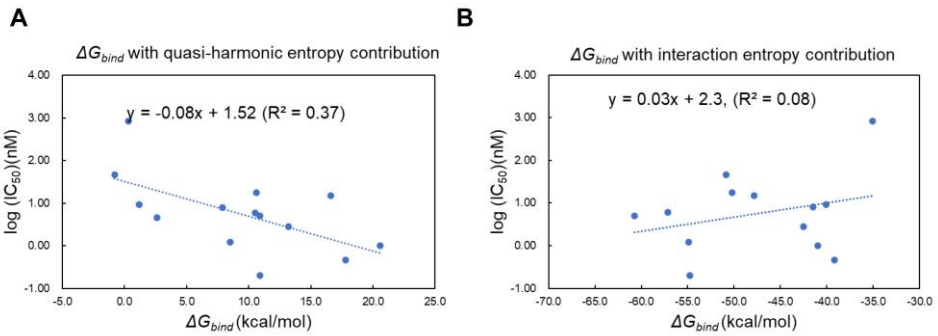

Figure S7. Including the entropy contribution in MM/GBSA binding energy did not improve the quality of binding affinity prediction for strong binders. (A) was with the entropy obtained using quasi-harmonic analysis; (B) was with the interaction entropy[1]. Actually, the entropy obtained using quasi-harmonic analysis even made the binding free energy worse.

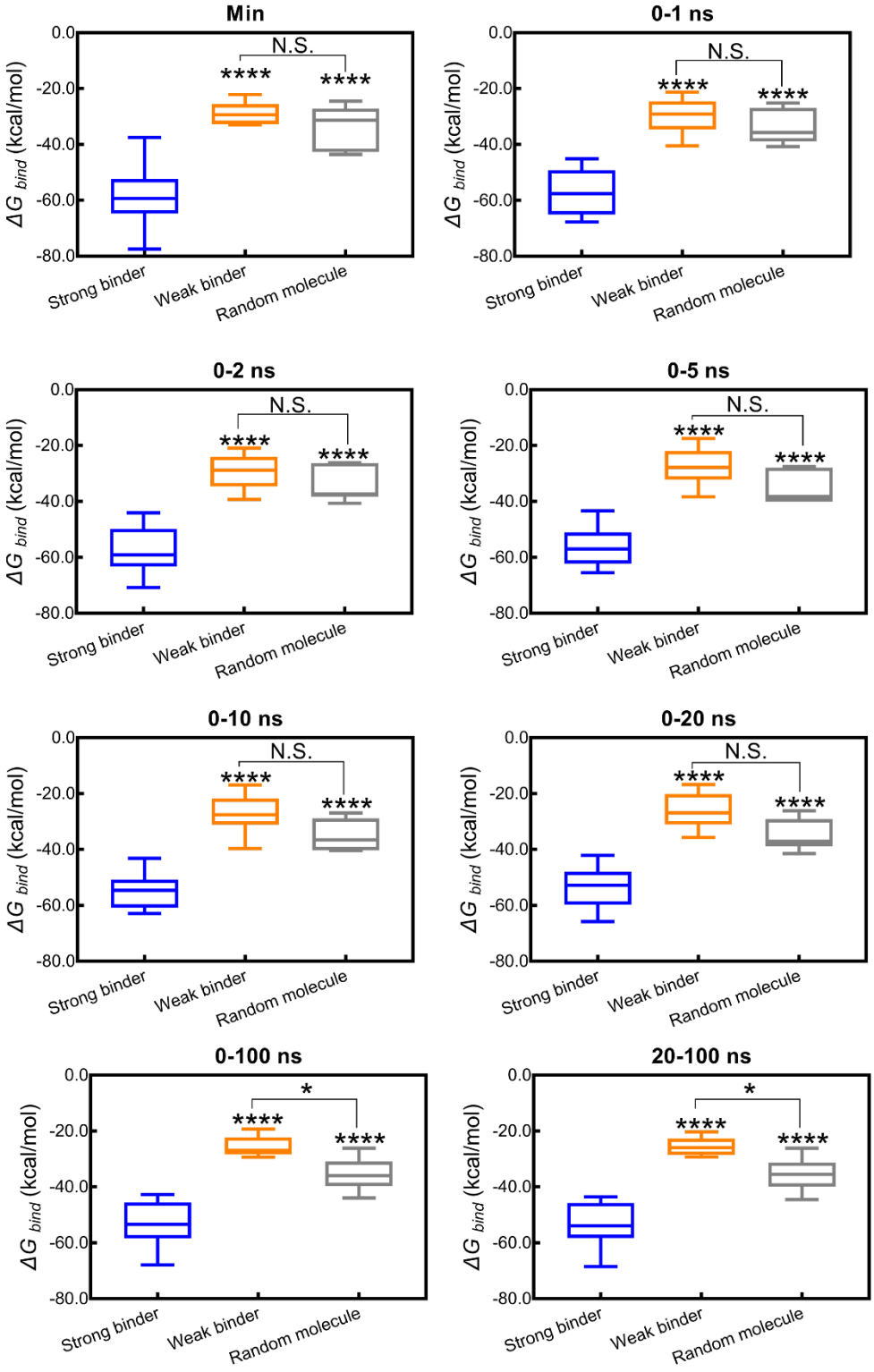

Figure S8. The distribution of the MM/GBSA binding free energy for strong binder (blue), weak binder (orange) and random molecule (grey). ΔG_{bind} predicted by MM/GBSA was taken from the lowest ΔG_{bind} among all the conformation for each

ligand in different timescale MD simulation. “Min” represents the single point MM/GBSA energy obtained based on the starting structure with a quick energy minimization. P ≥ 0.05, N.S.; * P < 0.05, **** P < 0.0001 vs. strong binder or as indicated (one-way ANOVA and Tukey’s multiple comparison test).

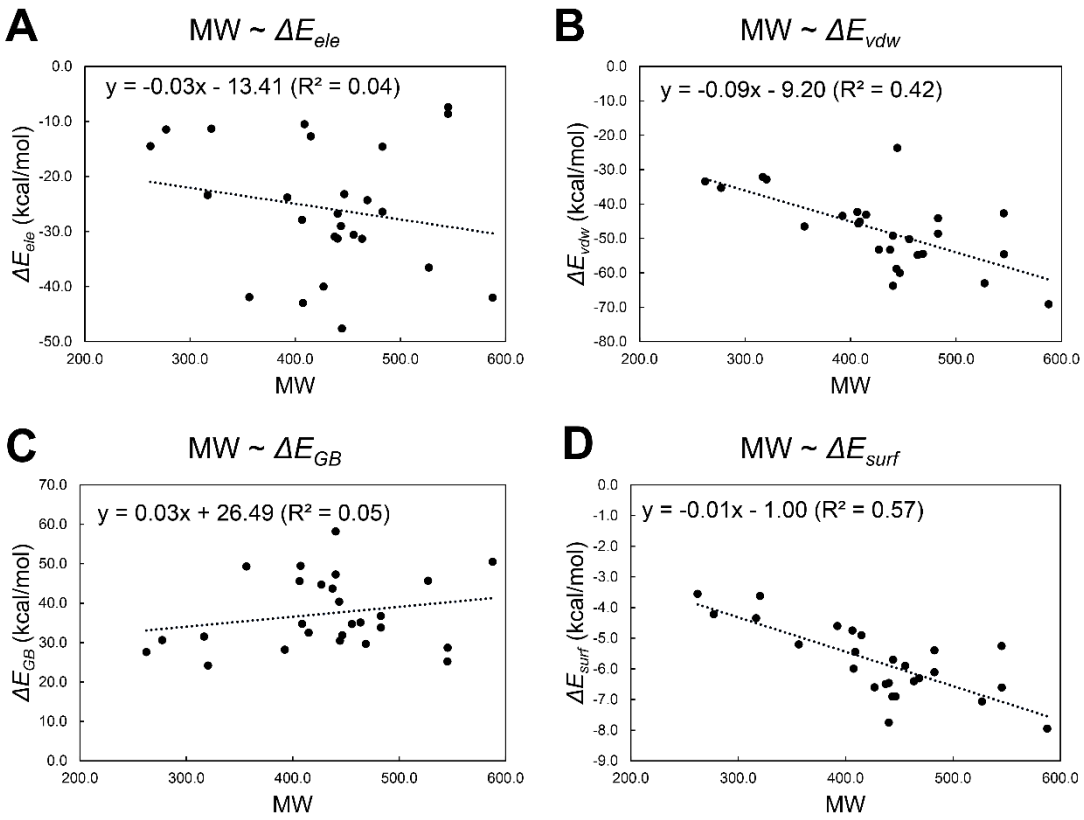

Figure S9. The MM/GBSA calculated ΔE_{vdw} (R^2 = 0.42) and ΔE_{surf} (R^2= 0.57) had stronger correlation with molecular weight (MW) of the ligand than that of ΔE_{ele} (R^2 = 0.04) and ΔE_{GB} (R^2= 0.05). (A) ΔE_{ele} refers to non-bonded electrostatic energy. (B) ΔE_{vdw} means van der Waals energy. (C) ΔE_{GB} is implicit polar solvation energy calculated using *GB* model. (D) ΔE_{surf} is non-polar solvation energy calculated by the solvent accessible surface area.

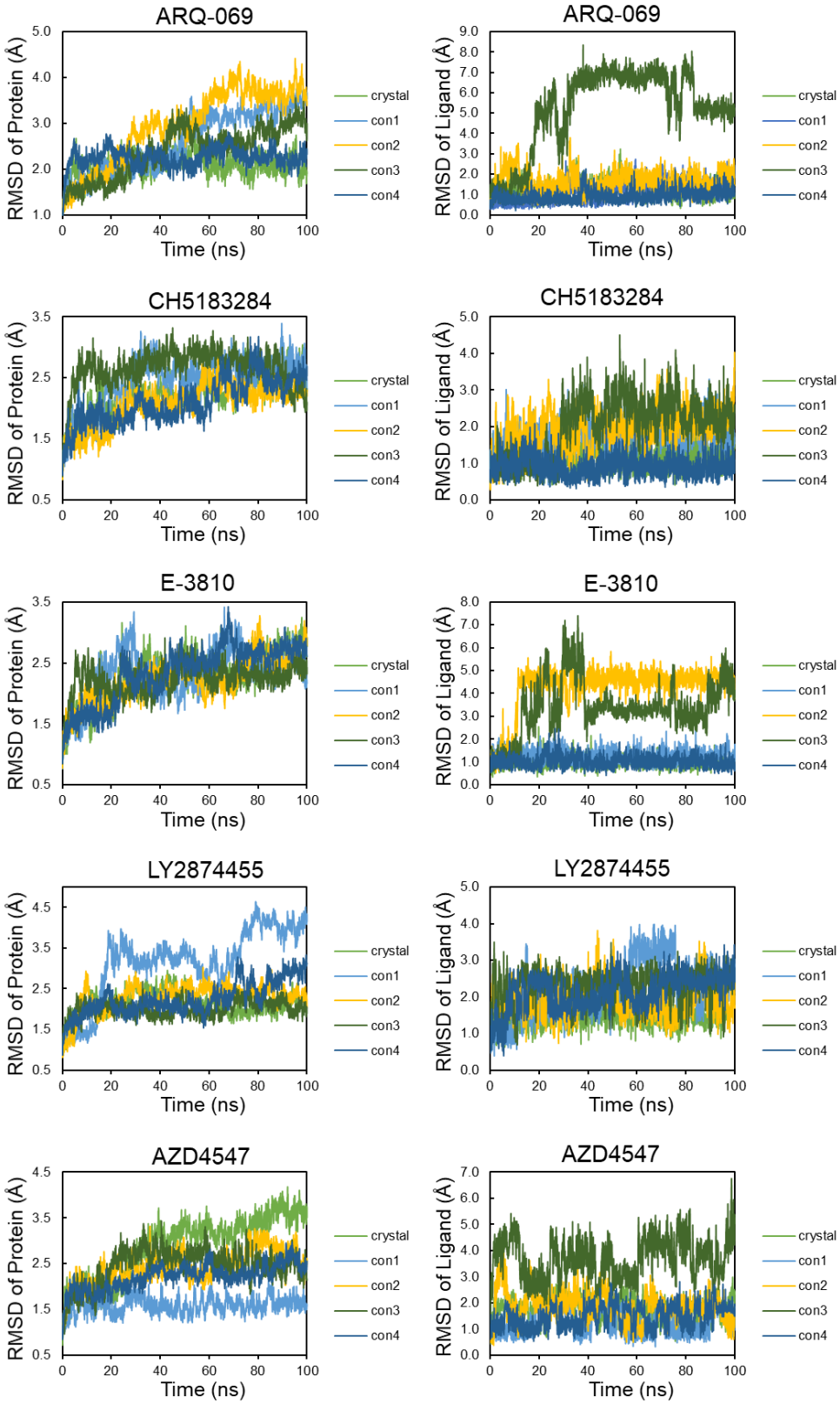
ARQ-069
RMSD of Protein (Å)
Time (ns)
ARQ-069
RMSD of Ligand (Å)
Time (ns)
CH5183284
RMSD of Protein (Å)
Time (ns)
CH5183284
RMSD of Ligand (Å)
Time (ns)
E-3810
RMSD of Protein (Å)
Time (ns)
E-3810
RMSD of Ligand (Å)
Time (ns)
LY2874455
RMSD of Protein (Å)
Time (ns)
LY2874455
RMSD of Ligand (Å)
Time (ns)
AZD4547
RMSD of Protein (Å)
Time (ns)
AZD4547
RMSD of Ligand (Å)
Time (ns)
crystal
con1
con2
con3
con4

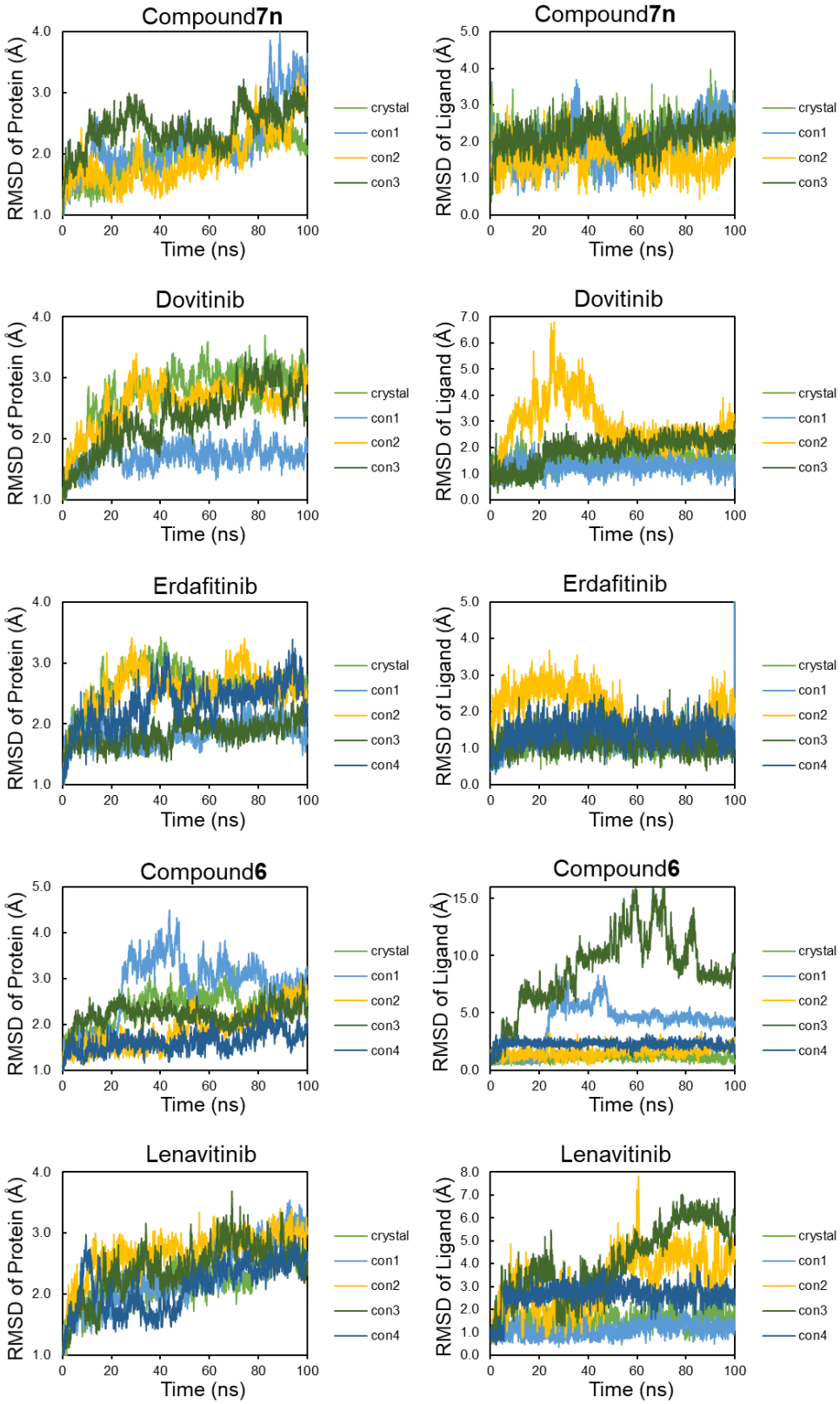
Compound7n
RMSD of Protein (Å)
Time (ns)
crystal
con1
con2
con3
Compound7n
RMSD of Ligand (Å)
Time (ns)
crystal
con1
con2
con3
Dovitinib
RMSD of Protein (Å)
Time (ns)
crystal
con1
con2
con3
Dovitinib
RMSD of Ligand (Å)
Time (ns)
crystal
con1
con2
con3
Erdafitinib
RMSD of Protein (Å)
Time (ns)
crystal
con1
con2
con3
con4
Erdafitinib
RMSD of Ligand (Å)
Time (ns)
crystal
con1
con2
con3
con4
Compound6
RMSD of Protein (Å)
Time (ns)
crystal
con1
con2
con3
con4
Compound6
RMSD of Ligand (Å)
Time (ns)
crystal
con1
con2
con3
con4
Lenavitinib
RMSD of Protein (Å)
Time (ns)
crystal
con1
con2
con3
con4
Lenavitinib
RMSD of Ligand (Å)
Time (ns)
crystal
con1
con2
con3
con4

Figure S10. The RMSD of protein backbone atoms (C, N, O, C_α, left panels) and ligand non-hydrogen atoms (right panels) against the starting structure of the 100 ns MD simulation.

2. Supplementary Tables

Table S1. The MM/GBSA binding free energy of ten ligands owning crystallographic structures. The energy is in unit of kcal/mol, and the RMSD is in Å. Values are reported in form of means ± standard deviation. The lowest energy and RMSD values are highlighted in bold (crystal structure not included).

Ligand conformation	Ligand PDB ID	Docking Method		MM/GBSA		
		Ranking	RMSD[A]	ΔG_{bind}	RMSD[A]	RMSD[B]
ARQ-069-crystal	3RHX (FGFR1)	/	0	-36.3 ± 0.5	1.3 ± 0.4	1.3 ± 0.4
ARQ-069-con1		1(Vina)	1.8	-37.2 ± 0.5	1.5 ± 0.4	1.3 ± 0.5
ARQ-069-con2		6(Vina)	4.6	-26.3 ± 2.5	4.8 ± 0.3	1.6 ± 0.4
ARQ-069-con3		2(Vina)	5.7	-20.2 ± 4.9	7.2 ± 0.7	6.1 ± 1.0
ARQ-069-con4		1(Glide)	0.3	**-39.0 ± 0.5**	**1.0 ± 0.4**	**1.0 ± 0.3**
CH5183284-crystal	5B7V (FGFR1)	/	0	-44.3 ± 0.4	0.8 ± 0.2	1.2 ±0.3
CH5183284-con1		1(Vina)	2.5	**-43.6 ± 2.7**	2.3 ± 0.2	1.9 ± 0.4
CH5183284-con2		2(Vina)	4.0	-33.4 ± 1.7	4.7 ± 0.6	2.3 ± 0.7
CH5183284-con3		3(Vina)	10.0	-31.8 ± 2.3	9.9 ± 0.2	2.0 ± 0.5
CH5183284-con4		1(Glide)	0.6	-43.3 ± 1.2	**0.9 ± 0.3**	**0.9 ± 0.3**
E-3810-crystal	4RWL (FGFR1)	/	0	-53.9 ± 1.4	1.5 ± 0.3	1.0 ± 0.2
E-3810-con1		2(Vina)	1.3	**-53.7 ± 0.3**	1.3 ± 0.3	1.3 ± 0.3
E-3810-con2		1(Vina)	5.2	-51.5 ± 1.3	1.5 ± 0.3	4.6 ± 0.3
E-3810-con3		3(Vina)	9.1	-32.3 ± 2.1	10.4 ± 0.8	3.7 ± 0.9
E-3810-con4		1(Glide)	0.9	-52.7 ±1.8	**1.2 ± 0.3**	**1.1 ± 0.3**
LY2874455-crystal	5JKG	/	0	-46.6 ± 1.3	1.1 ± 0.4	1.4 ± 0.3

LY2874455-con1	(FGFR4)	1(Vina)	1.7	-44.6 ± 1.0	1.9 ± 0.7	2.4 ± 0.6
LY2874455-con2		2(Vina)	2.0	**-46.5 ± 0.2**	2.0 ± 0.1	2.4 ± 0.4
LY2874455-con3		4(Vina)	7.4	-42.1 ± 3.4	7.8 ± 0.2	**1.9 ± 0.5**
LY2874455-con4		1(Glide)	2.2	-45.0 ± 0.9	**1.5 ± 0.4**	2.2 ± 0.4
AZD4547-crystal		/	0	-57.4 ± 0.7	1.6 ± 0.4	1.8 ± 0.4
AZD4547-con1	4RWK	2(Vina)	2.0	-58.3 ± 0.5	**1.5 ± 0.4**	**1.3 ± 0.5**
AZD4547-con2	(FGFR1)	1(Vina)	2.3	-53.5 ± 1.3	2.0 ± 0.4	1.8 ± 0.5
AZD4547-con3		6(Vina)	13.3	-45.5 ± 2.8	12.9 ± 0.5	3.7 ± 0.7
AZD4547-con4		1(Glide)	1.0	**-58.7 ± 0.6**	1.7 ± 0.5	1.5 ± 0.5
Compound**7n**-crystal		/	0	-52.0 ± 1.1	1.5 ± 0.3	2.2 ± 0.4
Compound**7n**-con1	4ZSA	2(Vina)	2.4	-49.1 ± 3.1	2.0 ± 0.4	2.0 ± 0.6
Compound**7n**-con2	(FGFR1)	1(Vina)	3.4	-43.4 ± 1.0	3.1 ± 0.2	**1.6 ± 0.4**
Compound**7n**-con3		1(Glide)	2.1	**-53.7 ± 1.1**	**1.6 ± 0.4**	2.2 ± 0.3
Dovitinib-crystal		/	0	-43.6 ± 5.3	1.2 ± 0.2	1.6 ± 0.4
Dovitinib-con1	5AM6	2(Vina)	1.0	-39.4 ± 0.5	**1.1 ± 0.2**	**1.3 ± 0.2**
Dovitinib-con2	(FGFR1)	1(Vina)	12.3	-34.5 ± 5.9	15.0 ± 0.7	3.0 ± 0.9
Dovitinib-con3		1(Glide)	10.6	**-59.2 ± 3.9**	10.1± 0.1	2.1 ± 0.3
Erdafitinib-crystal		/	0	-58.1 ± 1.3	0.9 ± 0.2	1.2 ± 0.3
Erdafitinib-con1		1(Vina)	1.9	-57.6 ± 1.0	1.9 ± 1.7	1.3 ± 1.7
Erdafitinib-con2	5EW8	2(Vina)	2.8	-56.0 ± 0.5	2.8 ± 0.1	**1.2 ± 0.3**
Erdafitinib-con3	(FGFR1)	7(Vina)	4.9	-50.8 ± 2.5	5.1 ± 0.1	2.0 ± 0.5
Erdafitinib-con4		1(Glide)	2.0	**-57.6 ± 0.3**	**1.3 ± 0.2**	1.5 ± 0.3

Compound**6**-crystal		/	0	-28.2 ± 1.0	1.4 ± 0.3	1.1 ± 0.3
Compound**6**-con1	5Z0S	8(Vina)	3.7	-21.3 ± 2.0	**5.5 ± 1.1**	4.9 ± 1.1
Compound**6**-con2	(FGFR1)	2(Vina)	4.6	-12.7 ± 4.8	9.9 ± 1.5	10.1 ± 2.4
Compound**6**-con3		1(Vina)	6.8	-23.6 ± 1.8	6.9 ± 0.3	**1.7 ± 0.5**
Compound**6**-con4		1(Glide)	6.6	**-28.4 ± 0.7**	10.0± 0.4	2.3 ± 0.3
Lenvatinib-crystal		/	0	-55.0 ± 0.4	1.3 ± 0.3	1.6 ± 0.4
Lenvatinib-con1	5ZV2	1(Vina)	4.3	-28.7 ± 5.4	8.1 ± 1.1	4.5 ± 1.4
Lenvatinib-con2	(FGFR1)	4(Vina)	5.2	-26.8 ± 4.0	7.0 ± 1.3	3.5 ± 1.1
Lenvatinib-con3		2(Vina)	5.7	-36.6 ± 0.3	5.4 ± 0.2	**1.1 ± 0.3**
Lenvatinib-con4		1(Glide)	2.5	**-50.0 ± 0.7**	**1.3 ± 0.2**	2.7 ± 0.3

RMSD^{A} was calculated against the PDB structure shown in second column.

RMSD^{B} was calculated against the starting structure of the production run of MD simulations.

Table S2. MM/GBSA correctly predicted the different binding affinity between the chiral enantiomers, ARQ-068 and ARQ-069, while Autodock Vina did not. Values are reported in form of means ± standard deviation. ΔG_{bind} predicted by MM/GBSA was taken from the lowest ΔG_{bind} among all the conformation for ARQ-068 and ARQ-069, respectively.

Ligand	**IC_{50} (nM) for FGFR1**[2]	**Autodock Vina**	**MM/GBSA**	
		ΔG_{bind} (kcal/mol)	**ΔG_{bind} (kcal/mol)**	**$RMSD^B$ (Å)**
ARQ-069(*S*)	840	-9.0	-37.2 ± 0.5	1.3 ± 0.5
ARQ-068(*R*)	>30000	-9.2	-34.9 ± 0.9	4.5 ± 0.8

In this study, we also encountered a pair of chiral enantiomers, the S enantiomer ARQ-069 and the R enantiomer ARQ-068. The former is active while the latter is not[2]. As shown in Table S2, ARQ-069 was predicted to have lower ΔG_{bind} with stable conformation during the MD, while ARQ-068 was unstable during the MD simulation, given the large $RMSD^B$ value of the compound.

Table S3. The detailed information of compounds considered in this study.

Molecular Name	Structure	Molecular Weight	Bioactivity on FGFR1
Strong binders			
CH5183284 (5B7V[3], LWJ; FGFR1 3mu)	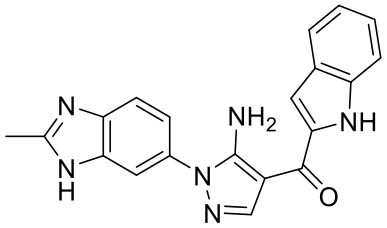	356.4	IC_{50} = 9.3 nM[3]
E-3810 (4RWL[4], 3ZC; FGFR1 3mu)	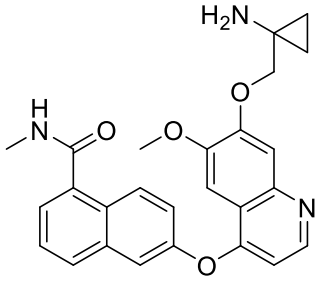	443.5	IC_{50} = 17.5 nM[5]
LY2874455 (5JKG[6], 6LF; FGFR4 WT)	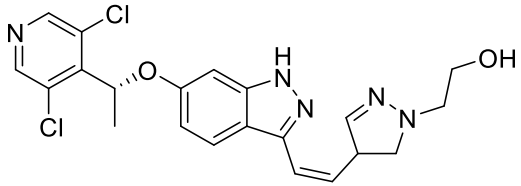	444.3	IC_{50} = 7.7 nM[7]

AZD4547 (4RWK[4], 66T;FGFR1 3mu)	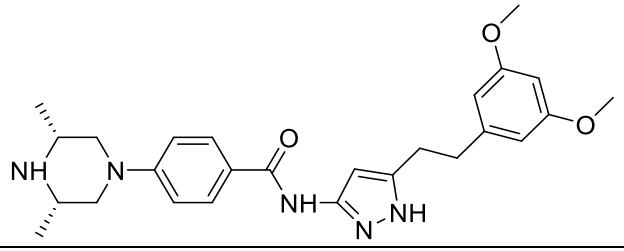	463.6	IC_{50} = 0.2 nM[8]
Compound**7n** (4ZSA[9], 4UT; FGFR1 2mu)	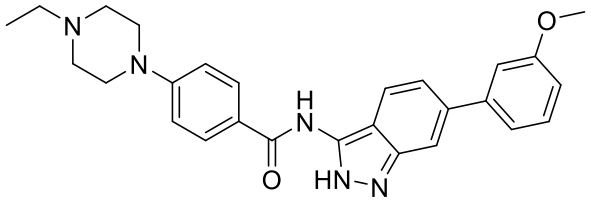	455.6	IC_{50} = 15 nM[9]
Dovitinib (5AM6[10], 38O; FGFR1 WT)	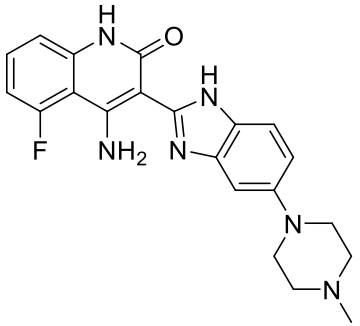	392.4	IC_{50} = 8 nM[11]

Erdafitinib (5EW8[12], 5SF; FGFR1 WT)	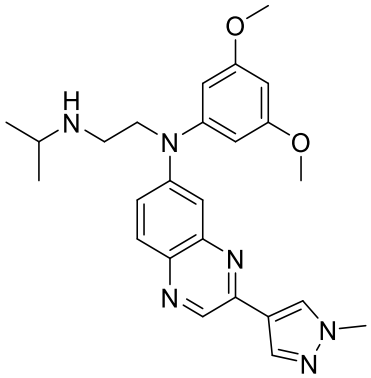	446.6	IC_{50} = 1.2 nM[13]
Lenvatinib (5ZV2[14], LEV; FGFR1 1mu)	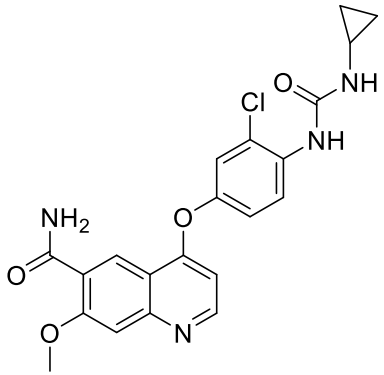	426.9	IC_{50} = 46 nM[15]

E-7090	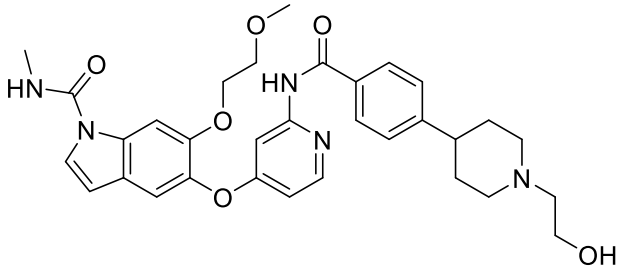	587.7	IC_{50} = 5 nM[16]
ASP-5878	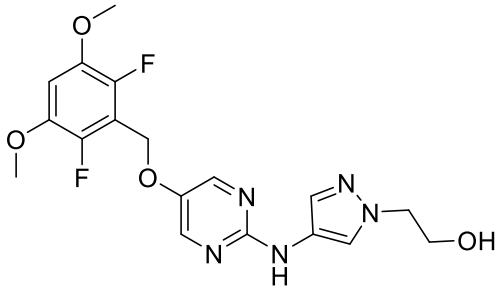	407.4	IC_{50} = 0.47 nM[17]
WO2013129369	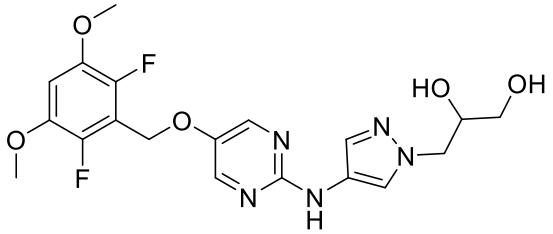	437.4	IC_{50} = 1 nM[18]

WO2014139465	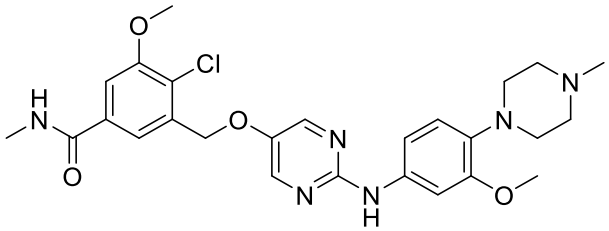	527.0	IC_{50} = 6 nM[19]
ARQ-087	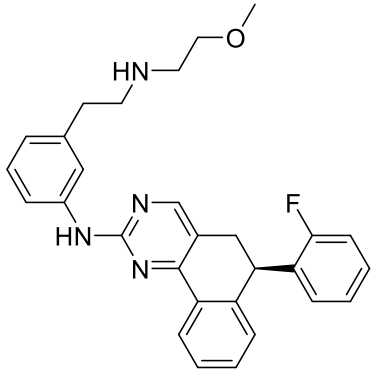	468.6	IC_{50} = 4.5[20]
Weak binders			
IJMS-6	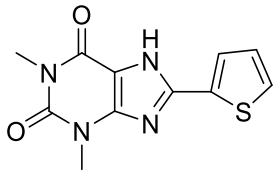	262.3	FGFR1 inhibition (%) at 10 μM=19.65 FGFR1 inhibition (%) at 50 μM=59.20

IJMS-42	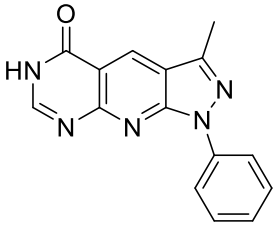	277.3	FGFR1 inhibition (%) at 10 μM=28.25 FGFR1 inhibition (%) at 50 μM=54.20
IJMS-92	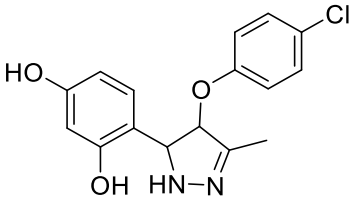	316.7	FGFR1 inhibition (%) at 10 μM=15.75 FGFR1 inhibition (%) at 50 μM=57.10
IJMS-96	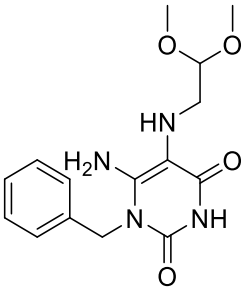	320.3	FGFR1 inhibition (%) at 10 μM=2.80 FGFR1 inhibition (%) at 50 μM=83.70
IJMS-99	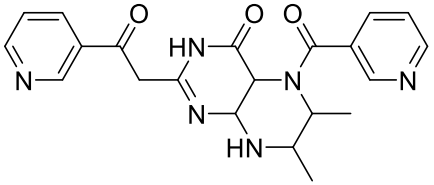	406.4	FGFR1 inhibition (%) at 10 μM=27.45 FGFR1 inhibition (%) at 50 μM =52.30[21]

Compound**6** (5Z0S[22], 960; FGFR1 2mu)	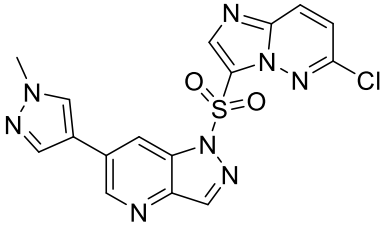	414.8	FGFR1 inhibition (%) at 10 μM=80.1[22]
Random molecules			
ZINC17342632	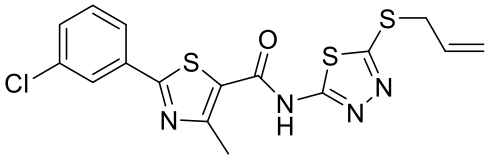	408.9	/
ZINC2542634	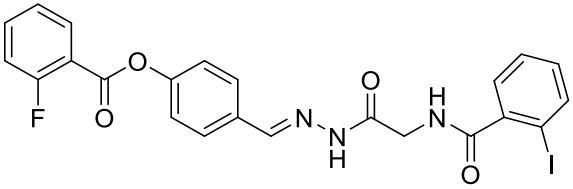	440.2	/
ZINC33357190	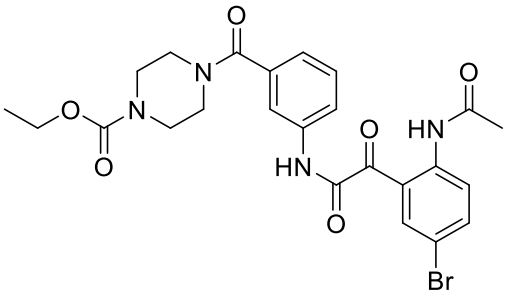	440.2	/

ZINC3510461	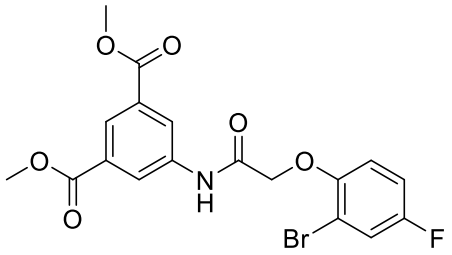	482.8	/
ZINC40583292	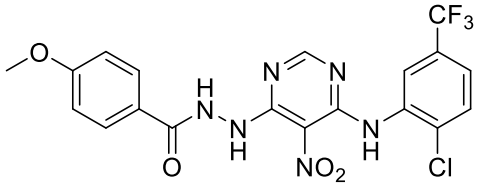	482.8	/
ZINC49405771	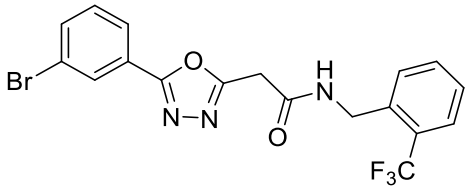	545.3	/
ZINC71886989	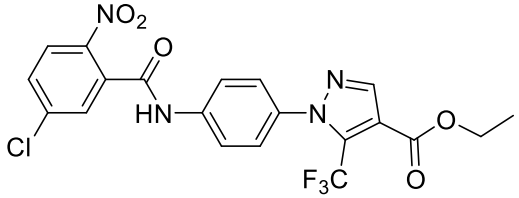	545.4	/
Chiral enantiomers			

ARQ-069 (3RHX[23], 3RH; FGFR1 2mu)	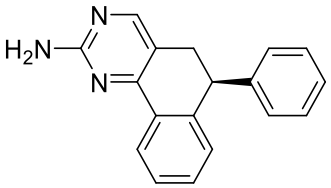	273.3	IC_{50} = 840 nM[23]
ARQ-068	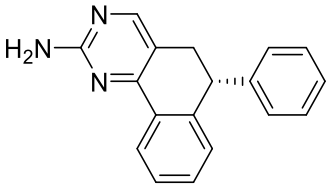	273.3	IC_{50}> 3 μM[23]

Table S4. The ΔG_{bind} calculated using MM/GBSA based on different timescales of MD simulation. Values are reported in form of means ± standard deviation. The error bars for 0-100 ns and 20-100 ns results were calculated using the standard deviation of the values of 0-20 ns, 20-40 ns, 40-60 ns, 60-80 ns and 80-100 ns MD simulation. Unit: kcal/mol.

	Min	**0-1 ns**	**0-2 ns**	**0-5 ns**	**0-10 ns**	**0-20 ns**	**20-40 ns**	**40-60 ns**	**60-80 ns**	**80-100 ns**	**0-100 ns**	**20-100 ns**
ARQ-069-crystal	-47.3	-40.4 ± 1.5	-38.2 ± 2.7	-38.5 ± 2.5	-37.7 ± 2.2	-36.6 ± 2.7	-37.0 ±2.5	-36.3 ± 2.4	-35.8 ± 2.6	-36.0 ± 2.7	-36.3 ± 0.5	-36.3 ± 0.5
ARQ-069-con1	-43.4	-49.1 ± 2.7	-49.5 ± 3.1	-47.8 ± 3.5	-46.7 ± 3.2	-44.7 ± 4.1	-37.2 ± 3.2	-37.0 ± 8.2	-36.6 ± 2.6	-37.9 ± 2.7	-38.7 ± 3.4	-37.2 ± 0.5
ARQ-069-con2	-23.2	-31.3 ± 1.9	-31.8 ± 1.8	-31.2 ± 3.0	-29.0 ± 3.0	-28.7 ± 3.2	-29.7 ± 3.2	-25.4 ± 4.0	-26.1 ± 3.8	-23.9 ± 3.5	-26.7 ± 2.4	-26.3 ± 2.5
ARQ-069-con3	-26.0	-30.5 ± 2.0	-29.9 ± 2.4	-26.9 ± 3.8	-25.2 ± 3.7	-24.4 ± 3.5	-17.9 ± 4.6	-17.3 ± 2.7	-17.9 ± 2.1	-27.5 ± 4.4	-21.0 ± 4.6	-20.2 ± 4.9
ARQ-069-con4	-47.7	-43.9 ± 2.9	-44.8 ± 2.8	-46.9 ± 3.3	-46.4 ± 2.9	-42.8 ± 4.7	-39.7 ± 2.6	-38.8 ± 3.1	-38.6 ± 2.8	-38.8 ± 3.0	-39.7 ± 1.8	-39.0 ± 0.5
CH5183284-crystal	-51.2	-47.0 ± 2.6	-46.5 ± 2.7	-44.7 ± 3.3	-45.3 ± 3.2	-44.9 ± 3.2	-44.8 ± 3.1	-44.1 ± 3.2	-43.8 ± 2.8	-44.5 ± 3.6	-44.4 ± 0.5	-44.3 ± 0.4
CH5183284-con1	-39.9	-42.3 ± 3.1	-40.6 ± 4.2	-39.4 ± 3.6	-38.2 ± 3.5	-37.6 ± 3.4	-47.3 ± 7.3	-42.5 ± 4.1	-43.6 ± 4.4	-40.9 ± 4.8	-42.4 ± 3.6	-43.6 ± 2.7
CH5183284-con2	-27.3	-39.0 ± 2.5	-39.2 ± 1.8	-38.2 ± 3.1	-37.4 ± 3.2	-37.0 ± 4.2	-32.7 ± 3.4	-34.5 ± 3.1	-29.6 ± 3.6	-30.4 ± 3.5	-32.8 ± 3.0	-31.8 ± 2.3
CH5183284-con3	-36.9	-33.6 ± 2.5	-34.8 ± 2.7	-34.7 ± 4.0	-35.4 ± 4.3	-35.3 ± 4.8	-31.6 ± 4.3	-32.9 ± 4.4	-33.4 ± 4.1	-35.7 ± 2.9	-33.8 ± 1.7	-33.4 ± 1.7
CH5183284-con4	-52.4	-43 ± 2.7	-41.0 ± 3.3	-41.0 ± 3.8	-42.3 ± 2.4	-41.5 ± 2.6	-44.8 ± 3.5	-43.1 ± 3.3	-41.9 ± 3.2	-43.6 ± 3.5	-43 ± 1.3	-43.3 ± 1.2
E-3810-crystal	-58.7	-51.3 ± 4.9	-51.3 ± 4.1	-51.6 ± 3.7	-50.6 ± 4.2	-50.4 ± 4.3	-51.8 ± 3.9	-54.0 ± 3.3	-54.7 ± 4.1	-55.1 ± 4.5	-53.2 ± 2.0	-53.9 ± 1.4
E-3810-con1	-56.0	-52.5 ± 3.4	-53.5 ± 3.0	-52.4 ± 3.4	-51.9 ± 3.9	-52.5 ± 4.2	-53.9 ± 3.3	-53.6 ± 3.4	-53.9 ± 3.5	-53.3 ± 2.7	-53.4 ± 0.6	-53.7 ± 0.3
E-3810-con2	-53.6	-44.4 ± 1.3	-44.7 ± 1.7	-44.3 ± 3.4	-43.3 ± 3.6	-48.4 ± 6.8	-51.1 ± 4.0	-52.5 ± 4.2	-49.8 ± 4.0	-52.5 ± 3.5	-50.9 ± 1.8	-51.5 ± 1.3
E-3810-con3	-45.6	-33.3 ± 5.6	-36.2 ± 6.0	-35.1 ± 7.6	-35.5 ± 5.7	-34.7 ± 5.9	-32.6 ± 5.0	-34.9 ± 3.8	-31.8 ± 5.6	-29.8 ± 4.6	-32.8 ± 2.1	-32.3 ± 2.1
E-3810-con4	-61.3	-52.3 ± 3.4	-53.1 ± 3.8	-53.1 ± 3.8	-51.6 ± 4.2	-51.4 ± 4.1	-50.5 ± 4.1	-52.1 ± 4.6	-54.6 ± 2.9	-53.7 ± 3.8	-52.5 ± 1.7	-52.7 ± 1.8
LY2874455-crystal	-50.7	-41.9 ± 3.2	-43.0 ± 4.3	-43.8 ± 3.5	-43.4 ± 3.5	-44.3 ± 3.5	-46.9 ± 3.0	-44.7 ± 3.5	-46.9 ± 3.5	-47.7 ± 3.0	-46.1 ± 1.5	-46.6 ± 1.3
LY2874455-con1	-44.7	-44.1 ± 2.8	-44.2 ± 2.8	-43.4 ± 3.1	-42.7 ± 2.9	-44.1 ± 3.7	-43.9 ± 3.8	-43.7 ± 3.0	-44.6 ± 3.2	-46.0 ± 3.7	-44.5 ± 0.9	-44.6 ± 1.0
LY2874455-con2	-46.4	-57.6 ± 3.4	-60.1 ± 4.2	-60.0 ± 3.2	-59.5 ± 2.5	-58.5 ± 3.3	-45.3 ± 7.4	-37.3 ± 5.8	-43.4 ± 3.9	-42.4 ± 4.6	-45.4 ± 7.9	-42.1 ± 3.4
LY2874455-con3	-45.1	-47.6 ± 3.8	-45.6 ± 4.0	-44.6 ± 3.2	-45.1 ± 3.5	-45.9 ± 3.7	-46.7 ± 4.2	-46.7 ± 3.7	-46.4 ± 3.5	-46.2 ± 3.1	-46.4 ± 0.4	-46.5 ± 0.2

LY2874455-con4	-47.6	-49.9 ± 3.1	-50.3 ± 2.5	-50.9 ± 2.4	-48.1 ± 3.9	-46.5 ± 4.0	-45.0 ± 3.2	-44.1 ± 3.2	-44.7 ± 3.4	-46.3 ± 3.1	-45.3 ± 1.0	-45.0 ± 0.9
AZD4547-crystal	-68.6	-62.4 ± 1.8	-60.4 ± 3.4	-58.5 ± 3.9	-58.6 ± 3.4	-59.1 ± 3.4	-56.4 ± 3.3	-57.9 ± 3.1	-57.6 ± 3.8	-57.8 ± 3.6	-57.8 ± 1.0	-57.4 ± 0.7
AZD4547-con1	-61.4	-60.1 ± 1.9	-58.7 ± 4.1	-59.2 ± 3.7	-58.3 ± 3.8	-57.4 ± 3.9	-58.6 ± 4.2	-58.1 ± 3.5	-58.7 ± 4.5	-57.7 ± 4.2	-58.1 ± 0.6	-58.3 ± 0.5
AZD4547-con2	-58.1	-67.0 ± 3.9	-67.0 ± 3.8	-64.5 ± 4.3	-62.9 ± 5.1	-59.9 ± 5.4	-53.1 ± 3.1	-55.4 ± 3.6	-52.3 ± 4.5	-53.2 ± 3.4	-54.8 ± 3.1	-53.5 ± 1.3
AZD4547-con3	-53.8	-46.2 ± 2.3	-42.5 ± 6.6	-41.6 ± 5.2	-41.4 ± 5.3	-41.7 ± 5.1	-42.9 ± 4.5	-44.8 ± 3.9	-44.7 ± 5.5	-49.5 ± 6.4	-44.7 ± 3.0	-45.5 ± 2.8
AZD4547-con4	-68.6	-65.8 ± 0.8	-64.1 ± 4.2	-60.0 ± 5.5	-58.8 ± 5.6	-59.4 ± 4.6	-58.6 ± 4.1	-59.5 ± 3.6	-58.4 ± 3.6	-58.2 ± 4.1	-58.8 ± 0.6	-58.7 ± 0.6
Compound**7n**-crystal	-59.1	-47.1 ± 3.6	-50.4 ± 4.5	-51.9 ± 4.6	-53.4 ± 5.0	-52.8 ± 4.7	-53.4 ± 4.3	-50.9 ± 4.1	-51.4 ± 3.9	-52.3 ± 3.7	-52.2 ± 1.0	-52.0 ± 1.1
Compound**7n**-con1	-55.7	-52.9 ± 3.5	-53.9 ± 3.4	-53.3 ± 4.1	-52.0 ± 3.9	-50.9 ± 4.6	-50.9 ± 4.8	-50.9 ± 4.2	-50.2 ± 3.9	-44.4 ± 3.9	-49.4 ± 2.8	-49.1 ± 3.1
Compound**7n**-con2	-59.3	-44.7 ± 2.2	-43.4 ± 2.9	-44.7 ± 3.6	-44.4 ± 3.5	-45.9 ± 3.5	-43.9 ± 3.9	-42.0 ± 3.3	-43.4 ± 3.9	-44.3 ± 4.2	-43.9 ± 1.4	-43.4 ± 1.0
Compound**7n**-con3	-66.4	-65.1 ± 4.2	-60.9 ± 7.2	-57.0 ± 6.9	-55.7 ± 5.6	-54.4 ± 5.2	-54.7 ± 4.1	-53.7 ± 5.4	-54.2 ± 4.2	-52.2 ± 4.6	-53.8 ± 1	-53.7 ± 1.1
Dovitinib-crystal	-35.8	-36.7 ± 2.4	-37.2 ± 2.3	-37.9 ± 2.5	-38.5 ± 2.1	-39.3 ± 1.9	-38.2 ± 2.6	-42.2 ± 2.7	-43.2 ± 2.3	-50.9 ± 4.2	-42.8 ± 5.0	-43.6 ± 5.3
Dovitinib-con1	-34.0	-38.4 ± 3.6	-37.2 ± 3.1	-37.7 ± 3.3	-38.0 ± 4.4	-38.6 ± 4.6	-40.0 ± 5.1	-39.0 ± 3.5	-38.9 ± 3.0	-39.6 ± 5.1	-39.2 ± 0.6	-39.4 ± 0.5
Dovitinib-con2	-37.5	-63.1 ± 4.5	-62.5 ± 4.0	-60.2 ± 5.2	-54.6 ± 2.7	-42.1 ± 2.9	-26.9 ± 2.7	-33.6 ± 4.2	-41.2 ± 4.1	-36.4 ± 3.9	-36.0 ± 6.2	-34.5 ± 5.9
Dovitinib-con3	-68.0	-66.8 ± 6.5	-66.2 ± 5.0	-66.0 ± 4.9	-67.5 ± 3.5	-65.4 ± 5.2	-53.7 ± 5.4	-59.2 ± 10.1	-61.8 ± 4.8	-62 ± 4.9	-60.4 ± 4.4	-59.2 ± 3.9
Erdafitinib-crystal	-62.7	-64.3 ± 1.9	-63.3 ± 2.2	-64.3 ± 2.9	-62.1 ± 2.7	-60.5 ± 3.0	-56.5 ± 2.8	-57.7 ± 3.7	-59.0 ± 4.1	-59.3 ± 6.6	-58.6 ± 1.5	-58.1 ± 1.3
Erdafitinib-con1	-77.4	-67.7 ± 4.0	-63.9 ± 5.3	-60.0 ± 6.3	-62.1 ± 2.9	-59.6 ± 3.0	-56.5 ± 2.7	-57.8 ± 2.9	-57.4 ± 2.7	-58.8 ± 3.4	-58.0 ± 1.2	-57.6 ± 1.0
Erdafitinib-con2	-50.8	-57.2 ± 5.3	-54.3 ± 5.4	-48.5 ± 6.2	-47.5 ± 10.6	-49.1 ± 16.0	-48.6 ± 6.5	-49.7 ± 7.5	-54.4 ± 4.5	-50.4 ± 7.8	-50.5 ± 2.3	-50.8 ± 2.5
Erdafitinib-con3	-68.9	-55.7 ± 3.9	-54.9 ± 3.8	-56.3 ± 3.4	-56.3 ± 3.8	-56.8 ± 3.4	-55.2 ± 3.7	-56.3 ± 3.9	-56.0 ± 4.1	-56.4 ± 4.2	-56.1 ± 0.6	-56.0 ± 0.5
Erdafitinib-con4	-67.2	-66.0 ± 3.0	-67.5 ± 3.5	-67.1 ± 3.9	-63.5 ± 6.3	-60.7 ± 6.0	-57.3 ± 3.3	-57.5 ± 3.6	-57.4 ± 3.4	-58.1 ± 3.5	-58.2 ± 1.4	-57.6 ± 0.3
Compound**6**-crystal	-31.2	-28.6 ± 2.0	-28.1 ± 1.8	-27.6 ± 2.1	-27.1 ± 4.5	-26.9 ± 4.1	-27.7 ± 3.4	-28.7 ± 3.8	-27.1 ± 4	-29.3 ± 4.3	-27.9 ± 1.0	-28.2 ± 1.0
Compound**6**-con1	-22.3	-32.7 ± 2.7	-33.1 ± 3.2	-29.0 ± 4.9	-27.4 ± 5.3	-24.6 ± 4.5	-18.7 ± 3.6	-21.6 ± 3.1	-21.1 ± 3.1	-23.6 ± 3.7	-21.9 ± 2.3	-21.2 ± 2.0

Compound**6**-con2	-25.1	-22.7 ± 2.1	-22.6 ± 2.3	-22.0 ± 2.4	-21.7 ± 5.1	-22.8 ± 5.4	-21.6 ± 4.0	-23.5 ± 4.3	-23.3 ± 3.4	-25.9 ± 4.1	-23.4 ± 1.6	-23.6 ± 1.8
Compound**6**-con3	-20.8	-18.0 ± 2.2	-18.2 ± 2.3	-19.0 ± 4.1	-17.6 ± 3.8	-16.9 ± 4.2	-16.5 ± 4.9	-16.3 ± 6.5	-6.2 ± 3.0	-11.9 ± 4.3	-13.6 ± 4.6	-12.7 ± 4.8
Compound**6**-con4	-28.8	-28 ± 2.2	-26.6 ± 3.0	-26.0 ± 3.4	-27.0 ± 3.3	-28.3 ± 3.7	-29.2 ± 2.4	-28.2 ± 3.4	-27.6 ± 3.3	-28.6 ± 3.3	-28.4 ± 0.6	-28.4 ± 0.7
Lenvatinib-crystal	-59.5	-58.7 ± 5.2	-61.2 ± 4.7	-57.0 ± 5.4	-56.5 ± 4.4	-55.5 ± 4.2	-55.1 ± 3.2	-54.5 ± 3.1	-55.3 ± 3.7	-55.3 ± 4.5	-55.1 ± 0.4	-55.0 ± 0.4
Lenvatinib-con1	-37.9	-37.7 ± 3.4	-37.0 ± 3.8	-36.4 ± 3.2	-35.6 ± 3.2	-35.7 ± 3.6	-36.5 ± 3.7	-36.2 ± 3.3	-36.8 ± 3.5	-36.7 ± 3.1	-36.4 ± 0.5	-36.6 ± 0.3
Lenvatinib-con2	-28.6	-37.6 ± 1.5	-36.3 ± 3.7	-33.5 ± 5.0	-31.8 ± 5.1	-30.6 ± 5.1	-32.7 ± 3.7	-25.3 ± 5.8	-24.3 ± 4.4	-24.7 ± 3.7	-27.5 ± 3.9	-26.7 ± 4.0
Lenvatinib-con3	-37.6	-30.3 ± 3.2	-30.9 ± 4.0	-28.2 ± 4.3	-26.4 ± 4.2	-24.7 ± 4.2	-24.3 ± 3.8	-25.2 ± 3.1	-29.2 ± 4.8	-36.0 ± 3.7	-27.9 ± 5.0	-28.7 ± 5.4
Lenvatinib-con4	-41.9	-34.1 ± 2.2	-34.3 ± 3.4	-34.0 ± 3.5	-40.5 ± 8.6	-45.4 ± 8.1	-50.6 ± 3.8	-49.7 ± 4.6	-50.4 ± 4	-49.1 ± 4.9	-49 ± 2.1	-49.9 ± 0.7
ASP-5878-con1	-60.8	-45.2 ± 2.7	-44.1 ± 2.9	-43.4 ± 3.2	-43.2 ± 3.5	-44.0 ± 3.4	-44.3 ± 4.5	-44.2 ± 2.9	-46.0 ± 3.4	-45.2 ± 4.3	-44.7 ± 0.8	-44.9 ± 0.8
ASP-5878-con2	-45.0	-31.7 ± 4.1	-32.0 ± 3.0	-37.3 ± 7.6	-40.1 ± 7.0	-42.0 ± 6.0	-44.1 ± 5.5	-44.9 ± 4.4	-45.0 ± 3.6	-46.7 ± 3.4	-44.5 ± 1.7	-45.2 ± 1.1
ASP-5878-con3	-43.4	-33.3 ± 3.4	-34.5 ± 3.2	-35.0 ± 3.2	-33.4 ± 3.0	-32.0 ± 3.4	-34.1 ± 3.9	-37.9 ± 3.6	-36.6 ± 3.0	-36.7 ± 3.6	-35.5 ± 2.4	-36.3 ± 1.6
E-7090-con1	-49.4	-52.4 ± 3.4	-54.0 ± 3.2	-56.2 ± 4.7	-55.0 ± 5.3	-55.6 ± 5.5	-52.0 ± 5.8	-51.0 ± 7.8	-49.1 ± 7.4	-48.8 ± 5.0	-51.3 ± 2.8	-50.2 ± 1.5
E-7090-con2	-70.7	-59.4 ± 7.1	-59.1 ± 6.6	-60.1 ± 6.6	-62.0 ± 6.7	-65.8 ± 8.1	-66.9 ± 6.5	-71.9 ± 9.1	-68.3 ± 7.8	-66.8 ± 4.9	-67.9 ± 2.4	-68.5 ± 2.4
WO2013129369-con1	-54.7	-50.4 ± 3.2	-50.6 ± 2.8	-51.0 ± 3.4	-49.8 ± 3.6	-48.7 ± 4.5	-46.9 ± 2.9	-47.1 ± 3.2	-47.2 ± 2.9	-46.6 ± 3.2	-47.3 ± 0.8	-47.0 ± 0.2
WO2013129369-con2	-48.0	-39.9 ± 2.4	-38.8 ± 2.9	-36.8 ± 4.0	-36.4 ± 3.5	-35.1 ± 3.4	-34.2 ± 3.8	-35.7 ± 3.7	-38.0 ± 5.4	-44.6 ± 4.1	-37.5 ± 4.2	-38.1 ± 4.6
WO2014139465-con1	-51.7	-58.8 ± 2.6	-60.3 ± 3.1	-57.8 ± 4.1	-58.3 ± 3.7	-59.5 ± 4.2	-60.4 ± 3.7	-60.3 ± 3.8	-61.5 ± 3.6	-61.3 ± 5.0	-60.6 ± 0.8	-60.8 ± 0.6
WO2014139465-con2	-53.5	-67.2 ± 4.2	-70.8 ± 5.5	-65.5 ± 8.9	-57.6 ± 11.0	-54.3 ± 9.4	-55.3 ± 5.2	-58.9 ± 3.9	-55.9 ± 6.5	-62.4 ± 5.7	-57.4 ± 3.3	-58.1 ± 3.3
ARQ-087-con1	-59.6	-47.9 ± 1.0	-49.0 ± 1.5	-51.1 ± 3.7	-51.7 ± 3.3	-52.8 ± 3.7	-55.8 ± 3.8	-54.8 ± 4.5	-55.2 ± 3.0	-55.9 ± 3.2	-54.9 ± 1.3	-55.4 ± 0.5
ARQ-087-con2	-55.7	-46.2 ± 3.8	-47.6 ± 4.6	-48.6 ± 5.4	-45.1 ± 6.1	-41.0 ± 6.7	-39.5 ± 4.3	-45.4 ± 4.6	-50.6 ± 7.1	-39.9 ± 7.0	-43.3 ± 4.7	-43.9 ± 5.3

IJMS-6-con1	-15.6	-23.1 ± 0.3	-23.4 ± 1.3	-22.5 ± 1.9	-21.8 ± 1.5	-21.6 ± 1.5	-21.4 ± 3.3	-18.1 ± 3.5	-18.7 ± 2.6	-18.7 ± 2.7	-19.7 ± 1.7	-19.2 ± 1.5
IJMS-6-con2	-27.6	-25.7 ± 0.7	-25.1 ± 1.0	-23.5 ± 2.1	-23.4 ± 2.1	-21.3 ± 7.3	-23.3 ± 4.0	-22.8 ± 2.4	-24.1 ± 2.3	-25.0 ± 2.1	-23.3 ± 1.4	-23.8 ± 1.0
IJMS-42-con1	-22.1	-21.3 ± 2.7	-20.9 ± 2.6	-17.5 ± 3.9	-16.8 ± 2.8	-15.1 ± 3.6	-20.2 ± 4.1	-20.1 ± 3.6	-20.2 ± 2.8	-20.9 ± 3.7	-19.3 ± 2.4	-20.3 ± 0.4
IJMS-42-con2	-21.5	-15.7 ± 2.8	-16.9 ± 2.9	-17.1 ± 3.0	-16.9 ± 2.2	-16.8 ± 2.6	-19.7 ± 3.5	-18.1 ± 3.0	-16.3 ± 3.0	-17.2 ± 3.0	-17.6 ± 1.3	-17.8 ± 1.4
IJMS-92-con1	-33.0	-30.8 ± 3.3	-30.7 ± 3.3	-30.1 ± 3.4	-27.8 ± 4.2	-26.9 ± 3.7	-26.6 ± 4.7	-26.0 ± 2.4	-31.7 ± 3.3	-29.0 ± 3.3	-28.0 ± 2.4	-28.3 ± 2.6
IJMS-92-con2	-27.3	-21.5 ± 2.9	-22.9 ± 2.8	-24.9 ± 3.2	-24.9 ± 3.0	-25.3 ± 2.7	-25.1 ± 2.4	-26.2 ± 2.3	-24.1 ± 2.2	-23.8 ± 2.4	-24.9 ± 1.0	-24.8 ± 1.1
IJMS-96-con1	-32.6	-40.2 ± 3.0	-38.6 ± 2.8	-38.4 ± 3.2	-36.5 ± 4.2	-35.7 ± 4.6	-22.7 ± 4.8	-23.3 ± 3.0	-23.2 ± 3.7	-25.0 ± 4.2	-26.0 ± 5.5	-23.5 ± 1.0
IJMS-96-con2	-30.6	-40.5 ± 5.9	-39.3 ± 6.2	-38.3 ± 5.5	-39.7 ± 5.2	-33.3 ± 8.1	-26.7 ± 5.3	-27.1 ± 4.1	-18.3 ± 5.8	-19.6 ± 4.1	-25.0 ± 6.1	-22.9 ± 4.6
IJMS-99-con1	-26.7	-12.6 ± 5.3	-11.3 ± 4.9	-8.5 ± 4.5	-10.3 ± 5.7	-11.7 ± 5.4	-10.6 ± 3.0	-18.7 ± 5.2	-19.3 ± 4.8	-25.3 ± 3.4	-17.1 ± 6.0	-18.5 ± 6.0
IJMS-99-con2	-15.6	-27.6 ± 1.7	-27.0 ± 3.9	-26.7 ± 3.3	-28.2 ± 4.1	-29.5 ± 4.1	-29.1 ± 4.1	-29.6 ± 4.4	-27.8 ± 4.0	-30.8 ± 3.9	-29.4 ± 1.1	-29.3 ± 1.2
ZINC17342632-con1	-24.5	-25.2 ± 3.9	-26.3 ± 3.1	-27.5 ± 3.3	-27.0 ± 4.3	-26.2 ± 4.1	-25.9 ± 4.0	-25.2 ± 5.2	-27.4 ± 2.7	-26.4 ± 2.9	-26.2 ± 0.8	-26.2 ± 0.9
ZINC2542634-con1	-42.7	-35.9 ± 1.9	-36.8 ± 2.2	-38.3 ± 3.2	-36.6 ± 3.9	-35.0 ± 3.9	-32.0 ± 4.1	-29.4 ± 5.0	-38.6 ± 5.8	-40.7 ± 4.0	-35.1 ± 4.7	-35.2 ± 5.4
ZINC33357190-con1	-29.2	-32.6 ± 1.2	-38.3 ± 6.2	-40.1 ± 4.8	-40.3 ± 4.6	-41.5 ± 4.4	-43.7 ± 5.0	-46.5 ± 5.1	-42.8 ± 4.9	-45.2 ± 5.4	-44.0 ± 2.0	-44.6 ± 1.7
ZINC3510461-con1	-31.3	-35.8 ± 2.8	-37.4 ± 3.3	-35.9 ± 3.2	-36.2 ± 3.3	-37.1 ± 3.4	-37.7 ± 3.6	-39.8 ± 3.1	-39.3 ± 3.0	-40.0 ± 3.0	-38.8 ± 1.3	-39.2 ± 1.0
ZINC40583292-con1	-43.6	-40.8 ± 4.9	-40.7 ± 4.1	-40.1 ± 3.2	-40.4 ± 2.8	-37.9 ± 4.2	-36.2 ± 4.1	-35.8 ± 4.3	-35.1 ± 3.3	-34.8 ± 4.0	-36.0 ± 1.2	-35.5 ± 0.6
ZINC49405771-con1	-27.1	-26.9 ± 3.1	-26.2 ± 2.5	-27.9 ± 4.0	-28.9 ± 3.9	-29.2 ± 3.5	-32.2 ± 2.6	-31.1 ± 3.0	-30.7 ± 3.4	-31.1 ± 4.3	-30.9 ± 1.1	-31.3 ± 0.7
ZINC71886989-con1	-40.1	-39.0 ± 2.6	-38.3 ± 2.4	-39.1 ± 2.4	-39.2 ± 3.0	-38.9 ± 3.2	-40.3 ± 3.2	-39.8 ± 2.7	-39.3 ± 3.1	-40.3 ± 3.1	-39.7 ± 0.6	-39.9 ± 0.5
ARQ-068-con1	-40.7	-38.5 ± 1.8	-39.7 ± 2.0	-38.6 ± 3.0	-39.1 ± 2.6	-39.8 ± 2.6	-33.9 ± 4.7	-33.4 ± 3.8	-27.6 ± 3.5	-30.2 ± 4.3	-33.0 ± 4.6	-31.3 ± 2.9
ARQ-068-con2	-26.8	-25.3 ± 1.5	-24.4 ± 2.1	-22.4 ± 2.6	-21.5 ± 3.0	-21.3 ± 3.1	-34.0 ± 5.5	-34.6 ± 4.7	-36.0 ± 4.7	-34.9 ± 4.2	-32.2 ± 6.1	-34.9 ± 0.9

Table S5. The ΔG_{bind} with entropy contribution obtained using quasi-harmonic analysis. Unit: kcal/mol.

	0-1 ns	0-2 ns	0-5 ns	0-10 ns	0-20 ns	20-40 ns	40-60 ns	60-80 ns	80-100 ns	0-100 ns	20-100 ns
ARQ-069-crystal	-12.6	-7.0	-3.3	-2.6	1.1	0.6	2.1	0.4	1.6	1.2	1.2
ARQ-069-con1	-21.5	-19.2	-13.2	-12.1	-6.8	1.7	-0.6	0.0	0.3	-1.1	0.3
ARQ-069-con2	-2.7	2.2	8.4	10.7	14.0	10.0	15.0	16.4	16.3	14.4	14.5
ARQ-069-con3	-2.5	1.4	8.5	11.3	15.1	22.1	21.2	22.1	12.5	18.6	19.5
ARQ-069-con4	-15.6	-13.3	-12.2	-11.7	-6.0	-1.2	-0.9	-0.9	-1.3	-2.1	-1.1
CH5183284-crystal	-16.8	-11.5	-2.5	-3.2	0.3	1.1	1.4	1.6	0.9	1.1	1.2
CH5183284-con1	-12.6	-6.3	2.8	4.5	9.0	-1.5	2.1	0.8	4.0	2.9	1.3
CH5183284-con2	-9.0	-5.0	3.0	4.3	9.0	14.0	12.8	19.0	14.9	13.9	15.2
CH5183284-con3	-3.9	-0.4	7.2	6.3	11.1	17.6	13.0	11.5	9.2	12.5	12.8
CH5183284-con4	-13.7	-7.0	0.8	-0.9	3.4	0.6	3.2	3.0	1.5	2.3	2.0
E-3810-crystal	-18.8	12.4	7.3	3.6	16.0	14.7	10.7	9.4	8.7	11.9	10.9
E-3810-con1	-20.0	-13.2	3.5	3.3	12.8	9.2	10.5	11.1	11.6	11.0	10.6
E-3810-con2	-11.7	-84.6	11.4	14.2	23.5	15.6	13.2	16.5	10.3	15.8	13.9
E-3810-con3	-1.8	2.6	18.9	18.6	37.2	40.7	31.5	39.9	38.1	37.5	37.6
E-3810-con4	-19.7	-13.0	1.1	4.5	16.2	17.2	13.8	9.6	10.3	13.4	12.7
LY2874455-crystal	-9.4	-3.3	7.3	8.6	16.7	13.7	14.5	13.3	11.4	13.9	13.2
LY2874455-con1	-11.9	-5.2	7.8	9.3	18.2	17.3	19.4	21.1	15.9	18.4	18.4
LY2874455-con2	-25.7	-22.3	-13.5	-12.2	-5.9	14.1	21.0	10.9	13.9	10.8	15.0
LY2874455-con3	-14.2	-3.9	10.6	9.4	16.8	14.9	13.4	13.7	15.1	-9.3	-15.8
LY2874455-con4	-17.3	-11.1	-0.1	5.6	16.5	16.8	15.2	15.9	12.4	15.4	15.1

AZD4547-crystal	-29.3	-18.6	-2.3	-2.6	10.3	12.7	11.6	10.5	12.0	11.4	11.7
AZD4547-con1	-28.0	-19.5	-5.9	-4.2	9.4	11.1	12.4	9.9	10.3	10.6	10.9
AZD4547-con2	-34.9	-27.4	-10.9	-9.6	9.8	18.1	15.3	19.8	18.9	16.4	18.0
AZD4547-con3	-12.5	0.6	20.3	22.2	37.9	37.7	35.6	36.9	31.3	35.9	35.4
AZD4547-con4	-33.6	-25.1	-6.4	-2.5	8.0	10.9	11.2	11.8	12.4	10.9	11.6
Compound**7n**-crystal	-14.1	-8.6	4.4	4.6	17.3	15.9	20.0	15.8	14.7	16.7	16.6
Compound**7n**-con1	-19.5	-13.1	2.5	3.7	16.3	16.2	15.7	21.2	24.0	18.7	19.3
Compound**7n**-con2	-12.5	-2.9	9.4	10.5	18.0	22.1	22.3	21.3	22.1	21.2	22.0
Compound**7n**-con3	-33.2	-20.2	0.0	1.8	14.5	14.8	15.0	15.3	15.1	14.9	15.0
Dovitinib-crystal	-5.6	-0.3	9.5	8.4	13.1	14.9	10.6	8.5	-2.3	9.0	7.9
Dovitinib-con1	-6.8	-0.2	8.5	9.2	13.7	12.5	13.7	13.3	13.2	13.3	13.2
Dovitinib-con2	-33.2	-27.3	-15.9	-9.5	11.0	25.1	18.7	8.0	16.1	15.8	17.0
Dovitinib-con3	-36.2	-31.0	-22.9	-25.0	-18.5	5.6	-10.3	-14.4	-14.3	-10.4	-8.4
Erdafitinib-crystal	-32.8	-24.6	-11.2	-8.5	5.8	12.5	9.3	6.5	5.7	8.0	8.5
Erdafitinib-con1	-36.2	-25.4	-6.9	-7.8	8.3	11.1	9.8	10.0	11.3	10.1	10.5
Erdafitinib-con2	-24.6	-14.3	8.6	9.6	21.0	18.3	20.7	10.0	23.4	18.7	18.1
Erdafitinib-con3	-23.2	-15.4	-1.9	-1.6	12.3	11.1	11.5	11.0	10.4	11.3	11.0
Erdafitinib-con4	-33.7	-28.4	-13.0	-8.2	8.6	12.5	11.4	9.3	9.2	10.2	10.6
Compound**6**-crystal	1.1	6.5	15.1	15.9	19.7	19.1	18.2	20.2	17.0	18.8	18.6
Compound**6**-con1	-2.2	2.3	14.6	16.5	23.7	33.0	27.3	27.6	24.5	27.2	28.1
Compound**6**-con2	7.3	12.6	21.7	22.1	24.7	26.4	25.4	25.2	22.7	24.9	24.9

Compound**6**-con3	12.8	17.8	25.6	27.4	32.7	32.3	35.9	44.7	35.6	36.3	37.1
Compound**6**-con4	2.6	9.2	19.1	18.1	20.6	18.3	21.2	19.5	19.3	19.8	19.6
Lenvatinib-crystal	-28.1	-25.8	-9.1	-7.5	-0.5	-2.1	-0.2	-0.6	-0.3	-0.7	-0.8
Lenvatinib-con1	-6.1	1.0	12.5	13.1	20.2	18.2	17.5	17.1	17.2	18.1	17.5
Lenvatinib-con2	-6.2	1.3	17.3	20.0	28.8	25.3	36.3	35.1	35.0	32.1	32.9
Lenvatinib-con3	1.1	7.1	22.4	25.9	36.5	37.1	39.9	29.5	20.1	32.6	31.6
Lenvatinib-con4	-3.0	2.5	13.7	10.2	12.9	5.2	4.4	3.9	7.5	6.8	5.3
ASP-5878-con1	-13.2	-4.9	10.1	10.3	19.5	20.5	19.3	16.4	17.7	18.7	18.5
ASP-5878-con2	0.6	7.3	21.6	18.8	26.7	21.1	18.0	19.0	13.2	19.6	17.8
ASP-5878-con3	-0.9	5.1	19.3	20.7	32.6	33.7	24.1	25.6	24.9	28.2	27.1
E-7090-con1	-17.5	-10.8	5.5	6.3	23.6	28.9	32.7	34.2	33.5	30.6	32.3
E-7090-con2	-25.0	-15.2	2.0	0.9	15.1	13.6	7.5	12.6	9.9	11.7	10.9
WO2013129369-con1	-17.0	-10.0	4.8	5.6	18.3	19.7	21.4	20.0	21.5	20.2	20.6
WO2013129369-con2	-7.9	1.4	20.2	21.6	34.2	35.8	35.8	34.6	17.9	31.7	31.0
WO2014139465-con1	-25.1	-19.1	1.1	0.8	13.1	9.9	10.5	9.6	12.1	11.1	10.5
WO2014139465-con2	-32.7	-28.5	-7.3	2.6	29.6	28.0	13.2	19.5	13.9	20.8	18.6
ARQ-087-con1	-15.9	-10.9	2.8	0.5	7.8	2.1	4.6	0.9	2.7	3.6	2.6
ARQ-087-con2	-13.8	-8.0	3.7	8.9	22.8	24.0	19.9	17.4	28.9	22.6	22.6

Table S6. The ΔG_{bind} with interaction entropy contribution.[1] Unit: kcal/mol.

	0-1 ns	0-2 ns	0-5 ns	0-10 ns	0-20 ns	20-40 ns	40-60 ns	60-80 ns	80-100 ns	0-100 ns	20-100 ns
ARQ-069-crystal	-38.8	-33.8	-35.2	-35.0	-33.8	-35.1	-33.8	-33.7	-33.7	-34.1	-34.1
ARQ-069-con1	-47.7	-48.4	-45.2	-44.0	-41.3	-35.2	-34.7	-34.8	-35.6	-35.6	-35.1
ARQ-069-con2	-29.7	-30.3	-27.5	-24.6	-24.9	-25.4	-21.2	-21.2	-20.6	-22.0	-21.4
ARQ-069-con3	-29.2	-28.8	-22.8	-21.8	-20.7	-13.0	-15.1	-15.7	-23.4	-16.8	-15.9
ARQ-069-con4	-41.1	-43.0	-44.7	-44.0	-38.4	-37.7	-36.8	-35.7	-36.4	-36.8	-36.6
CH5183284-crystal	-44.8	-43.4	-41.9	-42.5	-42.3	-41.5	-40.4	-39.7	-40.7	-40.7	-40.3
CH5183284-con1	-37.6	-36.0	-35.7	-34.3	-33.6	-38.2	-36.9	-38.6	-34.7	-34.6	-36.4
CH5183284-con2	-35.1	-35.8	-34.1	-32.2	-31.8	-27.5	-29.4	-24.9	-26.7	-27.6	-26.6
CH5183284-con3	-32.8	-32.9	-29.0	-29.8	-29.7	-24.5	-25.6	-25.9	-32.0	-27.5	-26.9
CH5183284-con4	-42.3	-39.9	-38.9	-40.1	-39.1	-39.8	-37.4	-39.0	-39.4	-38.2	-38.6
E-3810-crystal	-45.2	-47.0	-46.5	-45.1	-45.4	-47.6	-49.9	-50.7	-50.5	-48.5	-49.5
E-3810-con1	-49.3	-51.2	-48.9	-47.6	-48.5	-50.5	-49.5	-49.4	-49.3	-49.4	-49.7
E-3810-con2	-41.3	-36.4	-34.7	-34.7	-40.3	-43.2	-48.1	-42.7	-46.9	-43.4	-44.4
E-3810-con3	-32.4	-32.1	-30.6	-31.0	-27.7	-28.4	-30.7	-27.8	-24.9	-27.9	-28.0
E-3810-con4	-46.3	-48.2	-48.1	-46.8	-46.6	-45.3	-47.4	-50.4	-49.0	-47.7	-48.0
LY2874455-crystal	-37.5	-37.9	-38.0	-38.2	-39.9	-41.5	-40.2	-43.2	-44.2	-41.6	-42.3
LY2874455-con1	-43.1	-42.4	-39.8	-39.2	-39.7	-39.2	-38.6	-39.2	-39.8	-38.9	-38.9
LY2874455-con2	-57.2	-58.4	-57.4	-56.8	-55.7	-37.4	-31.6	-39.1	-38.5	-37.4	-36.1
LY2874455-con3	-45.5	-42.5	-41.3	-40.4	-41.0	-41.6	-42.6	-41.9	-42.4	-41.9	-42.0
LY2874455-con4	-48.9	-47.9	-46.4	-42.9	-41.7	-40.4	-40.0	-41.0	-41.3	-40.6	-40.3

AZD4547-crystal	-61.2	-58.3	-56.6	-55.8	-55.7	-52.8	-54.6	-54.5	-55.3	-54.5	-54.3
AZD4547-con1	-58.2	-55.8	-56.0	-54.9	-53.9	-54.7	-54.8	-54.9	-54.5	-54.5	-54.6
AZD4547-con2	-64.0	-60.4	-58.1	-56.7	-54.0	-47.9	-49.6	-46.8	-46.0	-48.7	-47.5
AZD4547-con3	-42.2	-38.9	-37.2	-37.7	-37.5	-39.6	-41.3	-40.1	-46.2	-39.9	-41.3
AZD4547-con4	-64.4	-62.6	-55.9	-53.5	-55.0	-54.8	-55.9	-52.9	-54.3	-54.3	-54.3
Compound**7n**-crystal	-44.2	-46.0	-47.6	-49.1	-48.1	-48.1	-47.3	-47.8	-48.6	-47.9	-47.8
Compound**7n**-con1	-49.4	-50.6	-49.3	-49.1	-47.5	-47.2	-47.8	-46.0	-39.9	-44.4	-43.6
Compound**7n**-con2	-38.8	-39.0	-41.0	-41.1	-42.5	-40.5	-38.4	-40.2	-39.7	-39.9	-39.3
Compound**7n**-con3	-59.9	-55.1	-52.1	-52.4	-50.4	-51.7	-49.8	-50.7	-47.9	-50.0	-49.9
Dovitinib-crystal	-35.2	-35.6	-36.4	-36.8	-37.1	-35.2	-38.9	-39.8	-46.9	-38.8	-39.5
Dovitinib-con1	-36.5	-34.8	-35.8	-35.4	-35.3	-37.5	-35.9	-35.9	-35.9	-35.8	-36.0
Dovitinib-con2	-61.2	-60.8	-57.0	-45.9	-29.2	-20.4	-27.5	-36.4	-30.0	-27.0	-26.9
Dovitinib-con3	-61.4	-61.8	-62.5	-63.8	-60.6	-48.2	-53.5	-58.5	-58.5	-54.6	-53.6
Erdafitinib-crystal	-62.9	-61.7	-61.5	-58.7	-56.8	-53.2	-53.4	-56.0	-56.1	-54.8	-54.3
Erdafitinib-con1	-66.4	-61.0	-53.2	-55.1	-53.9	-52.4	-54.4	-54.5	-55.4	-53.7	-53.6
Erdafitinib-con2	-49.3	-48.3	-44.5	-43.9	-42.6	-43.1	-44.3	-50.7	-45.7	-44.4	-44.9
Erdafitinib-con3	-52.7	-50.8	-53.2	-53.0	-53.2	-50.4	-52.8	-50.9	-51.9	-51.6	-51.3
Erdafitinib-con4	-63.7	-64.2	-63.6	-56.9	-54.2	-54.0	-54.3	-54.2	-55.1	-54.3	-54.3
Compound**6**-crystal	-26.9	-26.0	-26.1	-25.6	-25.1	-24.6	-25.8	-24.0	-25.4	-24.9	-25.0
Compound**6**-con1	-30.2	-29.9	-24.7	-23.0	-19.2	-12.8	-17.6	-17.6	-19.6	-15.7	-16.8
Compound**6**-con2	-18.9	-17.8	-17.0	-16.7	-18.4	-17.3	-18.4	-18.5	-21.7	-18.0	-18.0

Compound**6**-con3	-15.5	-15.6	-10.8	-10.9	-8.7	-10.1	-8.1	-1.1	-3.0	0.3	-1.1
Compound**6**-con4	-26.3	-23.9	-21.5	-22.5	-24.1	-24.9	-23.7	-24.2	-24.6	-23.8	-23.8
Lenvatinib-crystal	-53.5	-56.5	-52.4	-53.0	-51.2	-51.8	-49.7	-51.4	-51.7	-51.1	-51.1
Lenvatinib-con1	-33.1	-33.7	-32.4	-31.0	-30.9	-32.2	-31.4	-32.0	-32.6	-31.3	-31.9
Lenvatinib-con2	-33.8	-28.9	-23.2	-22.3	-21.8	-27.8	-8.6	-19.3	-19.9	-12.4	-11.8
Lenvatinib-con3	-29.7	-29.5	-23.0	-18.9	-18.3	-17.7	-20.9	-23.7	-32.8	-20.4	-21.0
Lenvatinib-con4	-30.0	-29.3	-29.5	-34.1	-39.7	-46.2	-43.2	-45.8	-42.3	-43.3	-44.2
ASP-5878-con1	-43.3	-41.1	-39.2	-36.9	-38.1	-38.5	-40.1	-39.2	-39.3	-38.8	-39.0
ASP-5878-con2	-28.5	-29.5	-30.8	-33.7	-36.7	-38.9	-40.7	-37.9	-42.2	-36.7	-37.2
ASP-5878-con3	-29.3	-31.2	-31.1	-29.4	-26.6	-24.1	-31.2	-32.1	-30.5	-26.3	-28.9
E-7090-con1	-48.8	-50.7	-51.0	-49.1	-48.7	-45.5	-41.6	-38.4	-42.2	-43.2	-41.8
E-7090-con2	-51.5	-50.1	-52.5	-54.8	-58.0	-60.9	-62.0	-59.7	-61.3	-60.1	-60.6
WO2013129369-con1	-49.3	-47.5	-46.5	-45.3	-43.0	-42.5	-39.5	-43.1	-40.4	-41.5	-41.4
WO2013129369-con2	-34.7	-34.2	-33.0	-31.4	-29.8	-25.6	-27.6	-27.5	-37.0	-25.7	-25.8
WO2014139465-con1	-56.8	-58.8	-55.4	-54.2	-55.5	-56.1	-57.0	-57.5	-57.1	-56.5	-56.9
WO2014139465-con2	-62.8	-66.5	-58.1	-48.8	-45.5	-49.7	-55.0	-50.8	-56.2	-50.4	-51.7
ARQ-087-con1	-46.0	-47.3	-45.5	-47.5	-47.7	-52.3	-51.8	-51.9	-53.1	-51.3	-52.3
ARQ-087-con2	-42.4	-43.1	-45.4	-40.9	-35.7	-34.4	-40.6	-45.0	-35.7	-37.8	-38.3

Table S7. The RMSD[A] (against the PDB structure) of each ligand at different timescales of the MD simulation. Values are reported in form of means ± standard deviation. The error bars for 0-100 ns and 20-100 ns results were calculated using the standard deviation of the values of 0-20 ns, 20-40 ns, 40-60 ns, 60-80 ns and 80-100 ns MD simulation. Unit: Å.

	Min	0-1 ns	0-2 ns	0-5 ns	0-10 ns	0-20 ns	20-40 ns	40-60 ns	60-80 ns	80-100 ns	0-100 ns	20-100 ns
ARQ-069-crystal	0.2	0.9 ± 0.2	0.9 ± 0.3	1.1 ± 0.3	1.2 ± 0.3	1.3 ± 0.4	1.3 ± 0.5	1.3 ± 0.4	1.2 ± 0.3	1.2 ± 0.3	1.3 ± 0.4	1.3 ± 0.4
ARQ-069-con1	1.7	0.9 ± 0.2	1.1 ± 0.2	1.1 ± 0.2	1.1 ± 0.2	1.0 ± 0.2	1.2 ± 0.4	1.4 ± 0.4	1.7 ± 0.3	1.7 ± 0.4	1.4 ± 0.5	1.5 ± 0.4
ARQ-069-con2	4.6	4.4 ± 0.2	4.5 ± 0.3	4.5 ± 0.3	4.6 ± 0.3	4.6 ± 0.3	4.7 ± 0.3	4.8 ± 0.3	4.8 ± 0.3	4.8 ± 0.3	4.8 ± 0.3	4.8 ± 0.3
ARQ-069-con3	5.7	6.2 ± 0.1	6.2 ± 0.2	6.4 ± 0.2	6.4 ± 0.2	6.6 ± 0.6	7.3 ± 0.9	7.6 ± 0.3	7.3 ± 0.5	6.6 ± 0.5	7.1 ± 0.7	7.2 ± 0.7
ARQ-069-con4	0.3	1.1 ± 0.2	1.1 ± 0.2	1.3 ± 0.2	1.3 ± 0.2	1.1 ± 0.3	1.0 ± 0.4	0.9 ± 0.3	1.0 ± 0.4	1.0 ± 0.3	1.0 ± 0.4	1.0 ± 0.4
CH5183284-crystal	0.4	0.7 ± 0.2	0.7 ± 0.2	0.7 ± 0.2	0.7 ± 0.2	0.7 ± 0.2	0.8 ± 0.2	0.9 ± 0.2	0.8 ± 0.2	0.8 ± 0.2	0.8 ± 0.2	0.8 ± 0.2
CH5183284-con1	2.4	2.1 ± 0.1	2.1 ± 0.1	2.1 ± 0.1	2.1 ± 0.1	2.1 ± 0.1	2.2 ± 0.2	2.3 ± 0.2	2.3 ± 0.2	2.3 ± 0.2	2.3 ± 0.2	2.3 ± 0.2
CH5183284-con2	3.9	3.6 ± 0.2	3.6 ± 0.2	3.8 ± 0.3	3.8 ± 0.3	3.7 ± 0.3	4.3 ± 0.7	5.0 ± 0.5	4.9 ± 0.4	4.8 ± 0.4	4.5 ± 0.7	4.7 ± 0.6
CH5183284-con3	10.0	9.9 ± 0.0	9.9 ± 0.1	9.9 ± 0.1	9.9 ± 0.1	9.9 ± 0.1	9.8 ± 0.1	9.7 ± 0.1	9.9 ± 0.2	10.2 ± 0.1	9.9 ± 0.3	9.9 ± 0.2
CH5183284-con4	0.5	0.8 ± 0.2	0.8 ± 0.2	0.9 ± 0.2	0.8 ± 0.2	0.9 ± 0.3	0.8 ± 0.3	1.0 ± 0.3	0.8 ± 0.2	0.9 ± 0.2	0.9 ± 0.3	0.9 ± 0.3
E-3810-crystal	0.3	1.1 ± 0.2	1.2 ± 0.2	1.4 ± 0.3	1.3 ± 0.3	1.3 ± 0.3	1.5 ± 0.4	1.5 ± 0.3	1.5 ± 0.3	1.5 ± 0.3	1.5 ± 0.3	1.5 ± 0.3
E-3810-con1	0.9	1.0 ± 0.2	1.1 ± 0.2	1.2 ± 0.2	1.1 ± 0.2	1.1 ± 0.2	1.2 ± 0.3	1.3 ± 0.3	1.3 ± 0.3	1.2 ± 0.3	1.2 ± 0.3	1.3 ± 0.3
E-3810-con2	5.1	3.8 ± 0.3	3.9 ± 0.3	3.8 ± 0.3	3.8 ± 0.4	2.6 ± 1.2	1.3 ± 0.3	1.6 ± 0.3	1.4 ± 0.3	1.5 ± 0.3	1.7 ± 0.8	10.4 ± 0.8
E-3810-con3	9.0	10.0 ± 0.2	10.0 ± 0.2	10.0 ± 0.2	10.0 ± 0.3	10.3 ± 0.5	11.2 ± 0.7	10.4 ± 0.2	10.2 ± 0.6	9.7 ± 0.6	10.4 ± 0.8	1.5 ± 0.3
E-3810-con4	0.9	1.2 ± 0.3	1.1 ± 0.2	1.1 ± 0.2	1.2 ± 0.3	1.2 ± 0.2	1.2 ± 0.3	1.2 ± 0.3	1.2 ± 0.2	1.1 ± 0.3	1.2 ± 0.3	1.2 ± 0.3
LY2874455-crystal	0.6	1.1 ± 0.2	1.2 ± 0.2	1.2 ± 0.2	1.2 ± 0.2	1.3 ± 0.3	1.2 ± 0.3	1.2 ± 0.2	1.2 ± 0.2	1.0 ± 0.5	1.2 ± 0.4	1.1 ± 0.4
LY2874455-con1	1.6	1.1 ± 0.2	1.1 ± 0.2	1.1 ± 0.2	1.1 ± 0.2	1.3 ± 0.4	1.5 ± 0.3	1.7 ± 0.6	2.7 ± 0.6	1.7 ± 0.3	1.8 ± 0.7	1.9 ± 0.7
LY2874455-con2	7.5	7.8 ± 0.1	7.8 ± 0.1	7.8 ± 0.1	7.9 ± 0.2	8.0 ± 0.2	7.8 ± 0.2	7.7 ± 0.2	7.8 ± 0.2	8.0 ± 0.2	7.8 ± 0.2	7.8 ± 0.2
LY2874455-con3	2.1	2.4 ± 0.2	2.2 ± 0.2	2.1 ± 0.2	2.1 ± 0.2	2.1 ± 0.2	1.9 ± 0.1	2.0 ± 0.1	2.0 ± 0.1	2.0 ± 0.1	2.0 ± 0.2	2.0 ± 0.1

LY2874455-con4	2.3	2.2 ± 0.2	2.3 ± 0.2	2.2 ± 0.2	2.1 ± 0.4	1.8 ± 0.5	1.5 ± 0.3	1.6 ± 0.3	1.6 ± 0.4	1.2 ± 0.3	1.5 ± 0.4	1.5 ± 0.4
AZD4547-crystal	0.3	2.0 ± 0.3	1.7 ± 0.5	1.5 ± 0.4	1.5 ± 0.4	1.5 ± 0.4	1.4 ± 0.4	1.6 ± 0.4	1.8 ± 0.2	1.5 ± 0.4	1.6 ± 0.4	1.6 ± 0.4
AZD4547-con1	1.6	1.1 ± 0.2	1.1 ± 0.2	1.1 ± 0.2	1.0 ± 0.2	1.1 ± 0.3	1.5 ± 0.4	1.5 ± 0.4	1.4 ± 0.4	1.4 ± 0.4	1.4 ± 0.4	1.5 ± 0.4
AZD4547-con2	2.7	1.8 ± 0.2	1.8 ± 0.2	2.2 ± 0.4	2.0 ± 0.5	2.0 ± 0.4	1.8 ± 0.3	1.8 ± 0.4	2.1 ± 0.4	2.1 ± 0.5	2.0 ± 0.4	2.3 ± 0.4
AZD4547-con3	13.5	13.1 ± 0.3	13.2 ± 0.2	13.3 ± 0.2	13.1 ± 0.4	12.9 ± 0.4	13.0 ± 0.5	13.1 ± 0.4	12.7 ± 0.5	12.9 ± 0.4	12.9 ± 0.5	2.0 ± 0.4
AZD4547-con4	0.9	1.2 ± 0.2	1.2 ± 0.2	1.1 ± 0.2	1.2 ± 0.4	1.2 ± 0.3	1.4 ± 0.4	1.8 ± 0.4	1.7 ± 0.4	1.9 ± 0.5	1.6 ± 0.5	1.7 ± 0.5
Compound**7n**-crystal	0.4	2.0 ± 0.3	2.0 ± 0.3	1.9 ± 0.3	1.9 ± 0.3	1.8 ± 0.3	1.6 ± 0.3	1.7 ± 0.3	1.4 ± 0.3	1.5 ± 0.3	1.6 ± 0.3	1.5 ± 0.3
Compound**7n**-con1	2.4	1.9 ± 0.2	1.9 ± 0.2	1.8 ± 0.2	1.8 ± 0.2	1.8 ± 0.2	1.9 ± 0.3	1.8 ± 0.2	2.0 ± 0.4	2.3 ± 0.4	2.0 ± 0.4	2.0 ± 0.4
Compound**7n**-con2	3.5	2.9 ± 0.1	3.0 ± 0.2	3.0 ± 0.2	3.1 ± 0.2	3.0 ± 0.2	3.1 ± 0.2	3.2 ± 0.2	3.0 ± 0.2	3.0 ± 0.2	3.1 ± 0.2	3.1 ± 0.2
Compound**7n**-con3	13.1	12.5 ± 0.2	12.5 ± 0.2	12.6 ± 0.1	12.6 ± 0.2	12.6 ± 0.2	13.0 ± 0.3	12.7 ± 0.2	12.6 ± 0.2	12.9 ± 0.2	12.8 ± 0.3	12.8 ± 0.3
Compound**7n**-con4	2.0	2.1 ± 0.1	2.0 ± 0.2	2.0 ± 0.3	1.9 ± 0.3	1.8 ± 0.3	1.8 ± 0.3	1.8 ± 0.3	1.6 ± 0.4	1.3 ± 0.3	1.7 ± 0.4	1.6 ± 0.4
Dovitinib-crystal	0.3	1.4 ± 0.3	1.4 ± 0.3	1.3 ± 0.3	1.2 ± 0.3	1.3 ± 0.3	1.1 ± 0.3	1.1 ± 0.3	1.3 ± 0.2	1.1 ± 0.2	1.2 ± 0.3	1.2 ± 0.2
Dovitinib-con1	0.7	1.3 ± 0.2	1.3 ± 0.2	1.4 ± 0.3	1.4 ± 0.3	1.4 ± 0.3	1.1 ± 0.2	1.1 ± 0.2	1.1 ± 0.2	1.1 ± 0.3	1.2 ± 0.3	1.1 ± 0.2
Dovitinib-con2	12.3	15.4 ± 0.2	15.4 ± 0.2	15.6 ± 0.3	15.5 ± 0.4	15.4 ± 0.6	15.1 ± 1.1	15.0 ± 0.5	14.9 ± 0.2	15.0 ± 0.3	15.1 ± 0.7	15.0 ± 0.7
Dovitinib-con3	10.6	10.4 ± 0.1	10.3 ± 0.2	10.3 ± 0.2	10.3 ± 0.2	10.3 ± 0.2	10.1 ± 0.1	10.0 ± 0.1	10.1 ± 0.1	10.1 ± 0.1	10.1 ± 0.3	10.1 ± 0.1
Compound**6**-crystal	0.5	1.2 ± 0.3	1.2 ± 0.3	1.2 ± 0.3	1.3 ± 0.3	1.3 ± 0.3	1.4 ± 0.3	1.5 ± 0.2	1.5 ± 0.3	1.3 ± 0.2	1.4 ± 0.3	1.4 ± 0.3
Compound**6**-con1	3.8	3.6 ± 0.2	3.7 ± 0.2	3.9 ± 0.3	4.0 ± 0.3	4.0 ± 0.3	5.9 ± 1.2	6.2 ± 1.4	5.2 ± 0.4	4.6 ± 0.4	5.2 ± 1.2	5.5 ± 1.1
Compound**6**-con2	4.7	6.7 ± 0.2	6.9 ± 0.3	7.0 ± 0.2	6.9 ± 0.2	7.0 ± 0.2	7.1 ± 0.2	7.0 ± 0.2	7.0 ± 0.2	6.6 ± 0.3	6.9 ± 0.3	6.9 ± 0.3
Compound**6**-con3	6.7	7.9 ± 0.3	7.7 ± 0.4	8.1 ± 0.6	8.1 ± 0.7	8.8 ± 1.0	8.7 ± 0.6	9.0 ± 1.4	11.1 ± 1.2	10.7 ± 0.8	9.7 ± 1.5	9.9 ± 1.5
Compound**6**-con4	6.6	10.2 ± 0.4	10.3 ± 0.4	10.4 ± 0.5	10.3 ± 0.4	10.1 ± 0.4	10.1 ± 0.3	10.1 ± 0.4	10.0 ± 0.3	9.9 ± 0.4	10.0 ± 0.4	10.0 ± 0.4
Erdafitinib-crystal	0.3	1.2 ± 0.2	1.3 ± 0.2	1.3 ± 0.3	1.1 ± 0.3	1.0 ± 0.3	0.9 ± 0.2	0.9 ± 0.2	0.9 ± 0.2	0.8 ± 0.2	0.9 ± 0.2	0.9 ± 0.2

Erdafitinib-con1	1.8	1.4 ± 0.1	1.4 ± 0.1	1.4 ± 0.2	1.6 ± 0.2	1.8 ± 0.3	1.9 ± 0.3	1.8 ± 0.2	1.8 ± 0.2	1.9 ± 3.3	1.9 ± 1.5	1.9 ± 1.7
Erdafitinib-con2	4.9	4.9 ± 0.2	5.0 ± 0.2	5.1 ± 0.2	5.2 ± 0.2	5.2 ± 0.2	5.2 ± 0.1	5.1 ± 0.1	5.0 ± 0.1	5.0 ± 0.1	5.1 ± 0.2	5.1 ± 0.1
Erdafitinib-con3	2.7	2.9 ± 0.1	2.9 ± 0.1	2.9 ± 0.1	2.8 ± 0.1	2.9 ± 0.1	2.9 ± 0.1	2.8 ± 0.1	2.7 ± 0.1	2.7 ± 0.1	2.8 ± 0.2	2.8 ± 0.1
Erdafitinib-con4	1.9	1.8 ± 0.3	1.9 ± 0.3	1.8 ± 0.3	1.6 ± 0.3	1.4 ± 0.3	1.3 ± 0.2	1.3 ± 0.2	1.3 ± 0.2	1.3 ± 0.2	1.3 ± 0.2	1.3 ± 0.2
Lenvatinib-crystal	0.5	1.3 ± 0.2	1.3 ± 0.2	1.4 ± 0.3	1.3 ± 0.3	1.3 ± 0.3	1.2 ± 0.3	1.3 ± 0.3	1.4 ± 0.3	1.2 ± 0.3	1.3 ± 0.3	1.3 ± 0.3
Lenvatinib-con1	4.3	6.5 ± 0.3	6.4 ± 0.2	6.7 ± 0.6	7.3 ± 0.8	7.5 ± 0.7	7.2 ± 0.7	7.5 ± 0.5	8.0 ± 1.1	9.4 ± 0.5	7.9 ± 1.1	8.1 ± 1.1
Lenvatinib-con2	5.2	5.1 ± 0.2	5.1 ± 0.3	5.3 ± 0.4	5.4 ± 0.4	5.4 ± 0.4	5.3 ± 0.3	6.8 ± 1.3	8.0 ± 0.5	7.9 ± 0.5	6.7 ± 1.4	7.0 ± 1.3
Lenvatinib-con3	5.6	5.0 ± 0.2	5.1 ± 0.2	5.1 ± 0.2	5.1 ± 0.2	5.1 ± 0.3	5.2 ± 0.2	5.4 ± 0.2	5.4 ± 0.2	5.5 ± 0.2	5.3 ± 0.3	5.4 ± 0.2
Lenvatinib-con4	2.4	2.5 ± 0.2	2.5 ± 0.2	2.5 ± 0.2	1.9 ± 0.7	1.5 ± 0.6	1.3 ± 0.2	1.3 ± 0.2	1.3 ± 0.2	1.3 ± 0.3	1.3 ± 0.4	1.3 ± 0.2

Table S8. The $RMSD^B$ (against the starting structure of the production MD simulation) of each ligand at different timescales of the MD simulation. Values are reported in form of means ± standard deviation. The error bars for 0-100 ns and 20-100 ns results were calculated using the standard deviation of the values of 0-20 ns, 20-40 ns, 40-60 ns, 60-80 ns and 80-100 ns MD simulation. Unit: Å.

	0-1 ns	**0-2 ns**	**0-5 ns**	**0-10 ns**	**0-20 ns**	**20-40 ns**	**40-60 ns**	**60-80 ns**	**80-100 ns**	**0-100 ns**	**20-100 ns**
ARQ-069-crystal	0.8 ± 0.2	1.0 ± 0.3	1.2 ± 0.3	1.2 ± 0.3	1.2 ± 0.3	1.3 ± 0.4	1.5 ± 0.4	1.2 ± 0.4	1.2 ± 0.4	1.3 ± 0.4	1.3 ± 0.4
ARQ-069-con1	0.5 ± 0.1	0.5 ± 0.1	0.6 ± 0.2	0.5 ± 0.2	0.6 ± 0.2	1.1 ± 0.4	1.1 ± 0.5	1.6 ± 0.3	1.4 ± 0.4	1.2 ± 0.5	1.3 ± 0.5
ARQ-069-con2	0.8 ± 0.3	1.1 ± 0.3	1.4 ± 0.5	1.9 ± 0.6	1.8 ± 0.7	1.5 ± 0.5	1.6 ± 0.4	1.6 ± 0.4	1.7 ± 0.4	1.6 ± 0.5	1.6 ± 0.4
ARQ-069-con3	1.2 ± 0.3	1.2 ± 0.3	1.2 ± 0.3	1.2 ± 0.3	1.8 ± 1.1	5.5 ± 1.1	6.9 ± 0.3	6.5 ± 0.8	5.5 ± 0.7	5.2 ± 2.0	6.1 ± 1.0
ARQ-069-con4	0.6 ± 0.1	0.7 ± 0.2	0.8 ± 0.3	0.8 ± 0.2	0.8 ± 0.2	0.9 ± 0.3	0.9 ± 0.3	1.0 ± 0.3	1.1 ± 0.3	0.9 ± 0.3	1.0 ± 0.3
CH5183284-crystal	1.0 ± 0.2	1.1 ± 0.3	1.1 ± 0.3	1.0 ± 0.3	1.1 ± 0.3	1.1 ± 0.3	1.2 ± 0.3	1.2 ± 0.3	1.3 ± 0.3	1.2 ± 0.3	1.2 ± 0.3
CH5183284-con1	0.9 ± 0.2	1.1 ± 0.3	1.3 ± 0.3	1.4 ± 0.4	1.5 ± 0.4	1.8 ± 0.5	1.9 ± 0.3	1.9 ± 0.3	1.9 ± 0.4	1.8 ± 0.4	1.9 ± 0.4
CH5183284-con2	0.7 ± 0.3	0.7 ± 0.3	1.1 ± 0.5	1.3 ± 0.6	1.5 ± 0.6	1.9 ± 0.5	1.9 ± 0.4	2.2 ± 0.5	2.2 ± 0.3	1.9 ± 0.5	2.0 ± 0.5
CH5183284-con3	0.8 ± 0.2	0.8 ± 0.2	1.0 ± 0.3	1.0 ± 0.3	1.0 ± 0.3	1.8 ± 0.9	2.6 ± 0.5	2.4 ± 0.4	2.3 ± 0.4	2.0 ± 0.8	2.3 ± 0.7
CH5183284-con4	0.8 ± 0.2	0.9 ± 0.2	0.9 ± 0.3	0.9 ± 0.3	1.0 ± 0.3	0.8 ± 0.2	1.0 ± 0.3	0.9 ± 0.2	0.9 ± 0.3	0.9 ± 0.3	0.9 ± 0.3
E-3810-crystal	0.9 ± 0.3	0.9 ± 0.2	0.9 ± 0.2	1.0 ± 0.2	1.0 ± 0.3	1.0 ± 0.2	1.0 ± 0.2	1.0 ± 0.2	1.0 ± 0.2	1.0 ± 0.2	1.0 ± 0.2
E-3810-con1	1.3 ± 0.3	1.3 ± 0.2	1.4 ± 0.3	1.3 ± 0.2	1.3 ± 0.2	1.3 ± 0.3	1.3 ± 0.3	1.3 ± 0.3	1.3 ± 0.3	1.3 ± 0.3	1.3 ± 0.3
E-3810-con2	1.0 ± 0.3	1.0 ± 0.2	1.1 ± 0.3	1.3 ± 0.4	2.8 ± 1.7	4.5 ± 0.4	4.7 ± 0.3	4.6 ± 0.3	4.6 ± 0.3	4.2 ± 1.1	4.6 ± 0.3
E-3810-con3	1.0 ± 0.3	1.0 ± 0.3	1.1 ± 0.3	1.2 ± 0.3	2.0 ± 1.1	4.5 ± 1.3	3.3 ± 0.3	3.4 ± 0.5	3.7 ± 0.8	3.4 ± 1.2	3.7 ± 0.9
E3810-con4	0.9 ± 0.2	1.0 ± 0.2	1.0 ± 0.2	1.0 ± 0.2	1.0 ± 0.2	1.1 ± 0.3	1.0 ± 0.2	1.0 ± 0.2	1.0 ± 0.2	1.0 ± 0.3	1.1 ± 0.3
LY2874455-crystal	1.2 ± 0.2	1.2 ± 0.2	1.1 ± 0.3	1.2 ± 0.3	1.3 ± 0.3	1.5 ± 0.2	1.6 ± 0.2	1.5 ± 0.3	1.2 ± 0.6	1.4 ± 0.4	1.4 ± 0.4
LY2874455-con1	0.9 ± 0.2	0.9 ± 0.2	1.0 ± 0.2	1.0 ± 0.2	1.4 ± 0.6	2.0 ± 0.3	2.3 ± 0.5	3.1 ± 0.5	2.4 ± 0.4	2.2 ± 0.7	2.4 ± 0.6
LY2874455-con2	1.7 ± 0.5	2.0 ± 0.5	1.7 ± 0.4	1.8 ± 0.4	1.8 ± 0.4	1.9 ± 0.5	2.1 ± 0.5	1.6 ± 0.3	2.0 ± 0.5	1.9 ± 0.5	1.9 ± 0.5
LY2874455-con3	1.3 ± 0.4	2.0 ± 0.8	2.0 ± 0.6	2.0 ± 0.5	2.2 ± 0.6	2.3 ± 0.4	2.3 ± 0.4	2.3 ± 0.4	2.4 ± 0.4	2.4 ± 0.4	2.4 ± 0.4

LY2874455-con4	1.0 ± 0.3	1.1 ± 0.3	1.1 ± 0.3	1.4 ± 0.5	1.8 ± 0.6	1.9 ± 0.4	2.2 ± 0.4	2.3 ± 0.4	2.5 ± 0.2	2.1 ± 0.5	2.2 ± 0.4
AZD4547-crystal	1.1 ± 0.4	1.4 ± 0.5	1.7 ± 0.4	1.8 ± 0.3	1.8 ± 0.4	1.9 ± 0.4	1.9 ± 0.4	1.6 ± 0.3	1.8 ± 0.4	1.8 ± 0.4	1.8 ± 0.4
AZD4547-con1	0.8 ± 0.2	0.8 ± 0.2	0.9 ± 0.2	0.9 ± 0.2	1.0 ± 0.3	1.5 ± 0.4	1.4 ± 0.5	1.1 ± 0.4	1.3 ± 0.4	1.2 ± 0.5	1.3 ± 0.5
AZD4547-con2	0.8 ± 0.2	1.0 ± 0.5	2.2 ± 1.1	2.1 ± 1.0	2.0 ± 0.8	2.0 ± 0.4	1.7 ± 0.6	1.8 ± 0.5	1.8 ± 0.4	1.9 ± 0.6	1.8 ± 0.5
AZD4547-con3	1.1 ± 0.2	1.2 ± 0.3	1.3 ± 0.3	1.4 ± 0.3	1.5 ± 0.4	1.6 ± 0.4	1.6 ± 0.4	1.7 ± 0.4	2.0 ± 0.4	1.7 ± 0.4	1.7 ± 0.4
AZD4547-con4	1.0 ± 0.2	1.1 ± 0.2	1.1 ± 0.2	1.3 ± 0.3	1.2 ± 0.3	1.3 ± 0.3	1.7 ± 0.4	1.5 ± 0.4	1.5 ± 0.6	1.4 ± 0.5	1.5 ± 0.5
Compound**7n**-crystal	2.5 ± 0.6	2.3 ± 0.6	2.1 ± 0.5	2.1 ± 0.5	2.0 ± 0.4	2.0 ± 0.4	2.0 ± 0.4	2.1 ± 0.4	2.4 ± 0.4	2.1 ± 0.4	2.2 ± 0.4
Compound**7n**-con1	1.2 ± 0.2	1.6 ± 0.5	1.5 ± 0.4	1.5 ± 0.4	1.4 ± 0.4	2.0 ± 0.5	1.7 ± 0.4	1.9 ± 0.4	2.6 ± 0.4	1.9 ± 0.6	2.0 ± 0.6
Compound**7n**-con2	1.0 ± 0.2	1.2 ± 0.4	1.2 ± 0.4	1.4 ± 0.5	1.4 ± 0.4	1.6 ± 0.4	1.8 ± 0.3	1.4 ± 0.4	1.4 ± 0.3	1.5 ± 0.4	1.6 ± 0.4
Compound**7n**-con3	2.2 ± 0.6	2.4 ± 0.5	2.6 ± 0.5	2.6 ± 0.5	2.6 ± 0.5	3.8 ± 0.8	4.0 ± 0.6	4.4 ± 0.7	3.2 ± 0.4	3.6 ± 0.9	3.9 ± 0.8
Compound**7n**-con4	0.9 ± 0.3	1.2 ± 0.5	1.7 ± 0.5	1.8 ± 0.4	1.9 ± 0.4	2.1 ± 0.3	2.1 ± 0.4	2.1 ± 0.3	2.3 ± 0.2	2.1 ± 0.4	2.2 ± 0.3
Dovitinib-crystal	1.2 ± 0.3	1.3 ± 0.3	1.1 ± 0.3	1.2 ± 0.3	1.3 ± 0.4	1.4 ± 0.3	1.6 ± 0.3	2.0 ± 0.3	1.5 ± 0.3	1.6 ± 0.4	1.6 ± 0.4
Dovitinib-con1	1.0 ± 0.2	1.0 ± 0.2	1.0 ± 0.3	1.1 ± 0.3	1.3 ± 0.3	1.2 ± 0.2	1.2 ± 0.2	1.3 ± 0.2	1.2 ± 0.2	1.3 ± 0.2	1.3 ± 0.2
Dovitinib-con2	0.9 ± 0.2	1.0 ± 0.2	1.3 ± 0.4	1.9 ± 0.8	2.6 ± 1.0	4.2 ± 0.8	2.8 ± 0.6	2.3 ± 0.3	2.5 ± 0.3	2.9 ± 0.9	3.0 ± 0.9
Dovitinib-con3	1.0 ± 0.3	1.0 ± 0.3	1.0 ± 0.3	1.0 ± 0.3	1.0 ± 0.3	1.9 ± 0.3	2.0 ± 0.3	2.2 ± 0.2	2.3 ± 0.2	1.9 ± 0.5	2.1 ± 0.3
Erdafitinib-crystal	0.7 ± 0.1	0.8 ± 0.1	0.8 ± 0.2	1.0 ± 0.3	1.1 ± 0.3	1.2 ± 0.3	1.3 ± 0.3	1.1 ± 0.3	1.2 ± 0.3	1.2 ± 0.3	1.2 ± 0.3
Erdafitinib-con1	0.7 ± 0.2	0.7 ± 0.1	0.8 ± 0.2	0.9 ± 0.3	1.1 ± 0.3	1.2 ± 0.2	1.2 ± 0.2	1.2 ± 0.2	1.4 ± 3.3	1.2 ± 1.6	1.3 ± 1.7
Erdafitinib-con2	1.3 ± 0.5	1.6 ± 0.5	2.0 ± 0.5	2.2 ± 0.5	2.4 ± 0.4	2.6 ± 0.3	2.0 ± 0.4	1.5 ± 0.2	1.9 ± 0.4	2.1 ± 0.5	2.0 ± 0.5
Erdafitinib-con3	1.1 ± 0.2	1.0 ± 0.3	1.0 ± 0.3	1.1 ± 0.3	1.1 ± 0.3	1.2 ± 0.3	1.3 ± 0.3	1.2 ± 0.3	1.1 ± 0.2	1.2 ± 0.3	1.2 ± 0.3
Erdafitinib-con4	0.7 ± 0.2	0.8 ± 0.2	0.8 ± 0.2	1.1 ± 0.3	1.3 ± 0.4	1.5 ± 0.3	1.6 ± 0.3	1.5 ± 0.3	1.5 ± 0.3	1.5 ± 0.3	1.5 ± 0.3
Compound**6**-crystal	0.9 ± 0.3	0.9 ± 0.3	0.9 ± 0.2	0.9 ± 0.3	0.9 ± 0.2	1.1 ± 0.3	1.2 ± 0.3	1.2 ± 0.3	1.0 ± 0.3	1.1 ± 0.3	1.1 ± 0.3

Compound**6**-con1	0.9 ± 0.2	0.8 ± 0.2	0.9 ± 0.2	1.0 ± 0.2	1.1 ± 0.2	5.0 ± 1.6	5.4 ± 1.0	5.0 ± 0.3	4.4 ± 0.3	4.1 ± 1.8	4.9 ± 1.1
Compound**6**-con2	1.5 ± 0.3	1.3 ± 0.3	1.3 ± 0.4	1.3 ± 0.4	1.3 ± 0.3	1.4 ± 0.5	1.5 ± 0.4	1.7 ± 0.4	2.0 ± 0.3	1.6 ± 0.5	1.7 ± 0.5
Compound**6**-con3	0.7 ± 0.2	0.8 ± 0.3	1.3 ± 0.8	2.2 ± 1.2	4.1 ± 2.2	7.8 ± 1.5	11.5 ± 1.8	11.7 ± 2.1	9.1 ± 1.5	8.8 ± 3.3	10.1 ± 2.4
Compound**6**-con4	1.2 ± 0.4	1.5 ± 0.5	1.8 ± 0.6	2.1 ± 0.5	2.3 ± 0.4	2.3 ± 0.2	2.3 ± 0.3	2.3 ± 0.3	2.2 ± 0.3	2.3 ± 0.3	2.3 ± 0.3
Lenvatinib-crystal	0.8 ± 0.2	0.8 ± 0.2	1.1 ± 0.3	1.3 ± 0.4	1.3 ± 0.3	1.4 ± 0.3	1.5 ± 0.4	1.7 ± 0.4	1.6 ± 0.4	1.5 ± 0.4	1.6 ± 0.4
Lenvatinib-con1	0.9 ± 0.2	0.8 ± 0.2	0.9 ± 0.2	1.0 ± 0.3	1.0 ± 0.3	0.9 ± 0.2	1.0 ± 0.3	1.3 ± 0.3	1.2 ± 0.3	1.1 ± 0.3	1.1 ± 0.3
Lenvatinib-con2	0.9 ± 0.2	1.0 ± 0.4	1.6 ± 0.8	2.1 ± 0.8	2.4 ± 1.0	2.2 ± 0.7	3.6 ± 1.1	4.3 ± 0.7	4.1 ± 0.7	3.3 ± 1.2	3.5 ± 1.1
Lenvatinib-con3	1.0 ± 0.2	1.1 ± 0.3	1.6 ± 0.8	2.1 ± 0.8	2.9 ± 0.9	3.0 ± 0.8	3.7 ± 0.8	5.4 ± 0.6	5.9 ± 0.5	4.1 ± 1.5	4.5 ± 1.4
Lenvatinib-con4	0.9 ± 0.2	0.9 ± 0.2	0.9 ± 0.2	1.7 ± 0.9	2.1 ± 0.8	2.8 ± 0.3	2.9 ± 0.3	2.6 ± 0.3	2.7 ± 0.4	2.6 ± 0.5	2.7 ± 0.3
ASP-5878-con1	0.9 ± 0.3	1.0 ± 0.2	1.2 ± 0.3	1.2 ± 0.3	1.2 ± 0.3	1.3 ± 0.3	1.0 ± 0.2	1.1 ± 0.2	1.1 ± 0.2	1.1 ± 0.3	1.1 ± 0.2
ASP-5878-con2	2.8 ± 0.4	2.7 ± 0.4	3.3 ± 1.0	3.8 ± 0.9	4.2 ± 0.8	5.3 ± 0.7	4.4 ± 0.2	4.1 ± 0.5	3.7 ± 0.2	4.3 ± 0.8	4.4 ± 0.8
ASP-5878-con3	1.4 ± 0.3	1.3 ± 0.4	1.4 ± 0.4	1.5 ± 0.3	1.4 ± 0.3	1.8 ± 0.4	2.2 ± 0.1	2.2 ± 0.1	2.2 ± 0.2	2.0 ± 0.4	2.1 ± 0.3
E-7090-con1	1.7 ± 0.2	1.4 ± 0.3	1.4 ± 0.3	1.3 ± 0.3	1.4 ± 0.4	2.2 ± 0.5	2.3 ± 0.5	2.3 ± 0.4	2.8 ± 0.5	2.2 ± 0.6	2.4 ± 0.5
E-7090-con3	1.9 ± 0.6	1.7 ± 0.5	1.5 ± 0.5	1.5 ± 0.4	1.8 ± 0.5	1.8 ± 0.5	2.1 ± 0.6	2.2 ± 0.5	2.3 ± 0.3	2.0 ± 0.5	2.1 ± 0.5
WO2013129369-con1	1.2 ± 0.2	1.3 ± 0.2	1.3 ± 0.3	1.5 ± 0.3	1.4 ± 0.3	1.5 ± 0.3	1.5 ± 0.3	1.5 ± 0.3	1.7 ± 0.3	1.5 ± 0.3	1.5 ± 0.3
WO2013129369-con2	0.9 ± 0.2	1.3 ± 0.5	1.6 ± 0.5	1.7 ± 0.4	1.8 ± 0.4	1.7 ± 0.3	1.6 ± 0.7	2.8 ± 0.6	3.2 ± 0.2	2.2 ± 0.8	2.3 ± 0.9
WO2014139465-con1	1.1 ± 0.2	1.0 ± 0.2	1.3 ± 0.4	1.4 ± 0.4	1.2 ± 0.4	1.1 ± 0.3	1.2 ± 0.2	1.2 ± 0.3	1.2 ± 0.3	1.2 ± 0.3	1.2 ± 0.3
WO2014139465-con2	2.4 ± 0.7	3.0 ± 0.8	3.3 ± 0.7	3.3 ± 0.6	3.7 ± 0.8	4.3 ± 0.8	3.6 ± 0.5	3.7 ± 0.6	4.5 ± 0.3	4.0 ± 0.7	4.0 ± 0.7
ARQ-087-con1	0.5 ± 0.1	0.5 ± 0.1	0.9 ± 0.4	1.2 ± 0.4	1.3 ± 0.3	1.4 ± 0.1	1.4 ± 0.1	1.4 ± 0.1	1.4 ± 0.1	1.4 ± 0.2	1.4 ± 0.1
ARQ-087-con2	0.6 ± 0.2	0.8 ± 0.2	0.8 ± 0.2	0.8 ± 0.2	0.9 ± 0.3	0.9 ± 0.2	0.8 ± 0.3	1.2 ± 0.4	1.1 ± 0.2	1.0 ± 0.4	1.0 ± 0.4

IJMS-6-con1	0.8 ± 0.3	0.8 ± 0.3	1.0 ± 0.4	1.2 ± 0.5	1.2 ± 0.5	2.1 ± 1.2	3.4 ± 0.8	2.8 ± 0.3	2.7 ± 0.4	2.4 ± 1.0	2.7 ± 0.9
IJMS-6-con2	0.9 ± 0.2	1.0 ± 0.3	1.0 ± 0.3	1.1 ± 0.3	1.0 ± 0.3	0.9 ± 0.2	1.0 ± 0.2	1.1 ± 0.2	1.1 ± 0.2	1.0 ± 0.3	1.0 ± 0.2
IJMS-42-con1	1.7 ± 0.7	2.0 ± 0.7	2.6 ± 1.2	2.2 ± 1.0	2.6 ± 1.0	3.8 ± 0.7	3.9 ± 0.5	3.9 ± 0.5	3.6 ± 0.5	3.6 ± 0.8	3.8 ± 0.6
IJMS-42-con2	1.4 ± 0.4	1.3 ± 0.3	1.3 ± 0.3	1.4 ± 0.4	1.6 ± 0.6	1.2 ± 0.3	1.9 ± 0.8	2.8 ± 0.7	1.7 ± 0.8	1.8 ± 0.8	1.9 ± 0.9
IJMS-92-con1	0.7 ± 0.2	0.8 ± 0.2	0.9 ± 0.3	1.4 ± 0.9	1.3 ± 0.7	1.0 ± 0.3	1.0 ± 0.3	0.8 ± 0.2	0.9 ± 0.3	1.0 ± 0.4	0.9 ± 0.3
IJMS-92-con2	1.3 ± 0.3	1.2 ± 0.3	1.1 ± 0.3	1.1 ± 0.3	1.1 ± 0.3	1.2 ± 0.4	1.1 ± 0.4	1.3 ± 0.3	1.4 ± 0.4	1.2 ± 0.4	1.3 ± 0.4
IJMS-96-con1	1.5 ± 0.1	1.5 ± 0.1	1.6 ± 0.1	1.6 ± 0.2	1.8 ± 0.3	3.4 ± 0.7	3.3 ± 0.6	3.8 ± 0.4	3.5 ± 0.7	3.1 ± 0.9	3.5 ± 0.6
IJMS-96-con2	1.2 ± 0.4	1.3 ± 0.3	1.5 ± 0.3	2.0 ± 0.8	2.2 ± 0.6	3.1 ± 1.3	4.4 ± 0.4	6.3 ± 1.4	6.7 ± 0.5	4.5 ± 2.0	5.1 ± 1.8
IJMS-99-con1	1.8 ± 0.4	2.8 ± 1.3	3.2 ± 1.3	3.9 ± 1.7	5.7 ± 2.5	11.2 ± 1.7	11 ± 1.0	11.4 ± 0.5	11.8 ± 0.4	10.2 ± 2.7	11.3 ± 1.1
IJMS-99-con2	1.0 ± 0.3	1.4 ± 0.5	1.8 ± 0.5	1.6 ± 0.5	1.3 ± 0.5	1.2 ± 0.4	1.2 ± 0.4	1.5 ± 0.6	1.1 ± 0.3	1.3 ± 0.5	1.3 ± 0.5
ZINC17342632-con1	1.0 ± 0.2	2.0 ± 1.3	3.2 ± 1.3	3.6 ± 1.0	3.8 ± 0.8	4.1 ± 0.3	6.1 ± 1.0	6.9 ± 0.9	9.2 ± 0.9	6.0 ± 2.1	6.6 ± 2.0
ZINC2542634-con1	1.5 ± 0.4	1.5 ± 0.4	1.6 ± 0.4	1.7 ± 0.5	2.3 ± 0.8	3.5 ± 0.7	3.4 ± 0.4	3.2 ± 0.3	3.3 ± 0.3	3.2 ± 0.7	3.4 ± 0.5
ZINC33357190-con1	0.9 ± 0.2	0.9 ± 0.2	1.1 ± 0.3	1.2 ± 0.2	1.3 ± 0.3	1.3 ± 0.2	1.7 ± 0.3	1.9 ± 0.3	2.0 ± 0.3	1.7 ± 0.4	1.8 ± 0.4
ZINC3510461-con1	2.4 ± 0.4	2.6 ± 0.3	2.6 ± 0.3	2.7 ± 0.2	2.8 ± 0.3	2.7 ± 0.3	2.6 ± 0.1	2.6 ± 0.2	2.5 ± 0.1	2.7 ± 0.2	2.6 ± 0.2
ZINC40583292-con1	1.2 ± 0.3	1.2 ± 0.3	1.6 ± 0.5	1.6 ± 0.5	1.8 ± 0.5	2.0 ± 0.4	2.3 ± 0.4	2.0 ± 0.4	1.9 ± 0.4	2.0 ± 0.4	2.1 ± 0.4
ZINC49405771-con1	1.5 ± 0.2	1.6 ± 0.3	2.2 ± 0.6	2.5 ± 0.6	2.5 ± 0.6	3.4 ± 0.7	2.9 ± 0.3	4.3 ± 0.5	5.5 ± 1.4	3.7 ± 1.3	4.0 ± 1.3
ZINC71886989-con1	1.1 ± 0.3	1.2 ± 0.3	1.1 ± 0.2	1.2 ± 0.3	1.3 ± 0.3	1.4 ± 0.3	1.3 ± 0.3	1.2 ± 0.3	1.2 ± 0.2	1.3 ± 0.3	1.3 ± 0.3
ARQ-068-con1	1.0 ± 0.3	1.0 ± 0.2	1.1 ± 0.3	1.2 ± 0.3	1.1 ± 0.3	1.7 ± 0.5	2.0 ± 0.6	2.3 ± 0.6	2.5 ± 0.6	1.9 ± 0.7	2.1 ± 0.6
ARQ-068-con2	0.7 ± 0.3	0.8 ± 0.3	1.0 ± 0.4	1.3 ± 0.7	1.6 ± 0.9	3.9 ± 1.3	4.7 ± 0.4	4.8 ± 0.4	4.8 ± 0.3	3.9 ± 1.5	4.5 ± 0.8

3. Abbreviations

GPU, graphics processing unit; FGFR, fibroblast growth factor receptor; MM/GBSA, molecular mechanics energies combined with the generalized Born and surface area continuum solvation; MD, molecular dynamics; RMSD, root-mean-square deviation; eEF2K, eukaryotic elongation factor 2 kinase; RTK, receptor tyrosine kinase; DFG, Asp-Phe-Gly; GAFF, generalized Amber force field; TIP3P, transferable intermolecular potential with 3 points; NVT, constant number (N), volume (V), and temperature (T); NPT, constant number (N), pressure (P), and temperature (T); Min, minimization; N.S., no significance; ANOVA, Analysis of variance; MW, molecular weight.

References

S1 L. Duan, X. Liu, and J. Z. Zhang, *J Am Chem Soc*, 2016, **138**, 5722.

S2 S. Eathiraj, R. Palma, M. Hirschi, E. Volckova, E. Nakuci, J. Castro, C. R. Chen, T. C. K. Chan, D. S. France, and M. A. Ashwell, *J. Biol. Chem.*, 2011, **286**, 20677.

S3 Y. Nakanishi, N. Akiyama, T. Tsukaguchi, T. Fujii, K. Sakata, H. Sase, T. Isobe, K. Morikami, H. Shindoh, T. Mio, H. Ebiike, N. Taka, Y. Aoki, and N. Ishii, *Mol. Cancer Ther.*, 2014, **13**, 2547.

S4 C. D. Sohl, M. R. Ryan, B. B. Luo, K. M. Frey, and K. S. Anderson, *ACS Chem. Biol.*, 2015, **10**, 1319.

S5 E. Bello, G. Colella, V. Scarlato, P. Oliva, A. Berndt, G. Valbusa, S. C. Serra, M. Incalci, E. Cavalletti, R. Giavazzi, G. Damia, and G. Camboni, *Cancer Res.*, 2011, **71**, 1396.

S6 D. C. Wu, M. Guo, M. A. Philips, L. Z. Qu, L. Y. Jiang, J. Li, X. J. Chen, Z. C. Chen, L. Chen, and Y. H. Chen, *PLOS ONE*, 2016, **11**, e0162491.

S7 G. S. Zhao, W. Y. Li, D. H. Chen, J. R. Henry, H. Y. Li, Z. G. Chen, M. Zia-Ebrahimi, L. Bloem, Y. Zhai, K. Huss, S. B. Peng, and D. J. McCann, *Mol. Cancer Ther.*, 2011, **10**, 2200.

S8 P. R. Gavine, L. Mooney, E. Kilgour, A. P. Thomas, K. Al Kadhimi, S. Beck, C. Rooney, T. Coleman, D. Baker, M. J. Mellor, A. N. Brooks, and T. Klinowska, *Cancer Res.*, 2012, **72**, 2045.

S9 J. Liu, X. Peng, Y. Dai, W. Zhang, S. M. Ren, J. Ai, M. Y. Geng, and Y. X. Li, *Org. Biomol. Chem.*, 2015, **13**, 7643.

S10 T. D. Bunney, S. Z. Wan, N. Thiyagarajan, L. Sutto, S. V. Williams, P. Ashford,

H. Koss, M. A. Knowles, F. L. Gervasio, P. V. Coveney, and M. Katan, *Electromagn. Biol. Med.*, 2015, **2**, 194.

S11 S. Trudel, Z. H. Li, E. Wei, M. Wiesmann, H. Chang, C. Chen, D. Reece, C. Heise, and A. K. Stewart, *Blood*, 2005, **105**, 2941.

S12 H. Patani, T. D. Bunney, N. Thiyagarajan, R. A. Norman, D. Ogg, J. Breed, P. Ashford, A. Potterton, M. Edwards, S. V. Williams, G. S. Thomson, C. S. M. Pang, M. A. Knowles, A. L. Breeze, C. Orengo, C. Phillips, and M. Katan, *Oncotarget*, 2016, **7**, 24252.

S13 T. P. S. Perera, E. Jovcheva, L. Mevellec, J. Vialard, D. De Lange, T. Verhulst, C. Paulussen, K. Van De Ven, P. King, E. Freyne, D. C. Rees, M. Squires, G. Saxty, M. Page, C. W. Murray, R. Gilissen, G. Ward, N. T. Thompson, D. R. Newell, N. Cheng, L. Xie, J. Yang, S. J. Platero, J. D. Karkera, C. Moy, P. Angibaud, S. Laquerre, and M. V. Lorenzi, *Mol. Cancer Ther.*, 2017, **16**, 1010.

S14 M. Matsuki, T. Hoshi, Y. Yamamoto, M. Ikemori Kawada, Y. Minoshima, Y. Funahashi, and J. Matsui, *Cancer Med.*, 2018, **7**, 2641.

S15 J. Matsui, Y. Yamamoto, Y. Funahashi, A. Tsuruoka, T. Watanabe, T. Wakabayashi, T. Uenaka, and M. Asada, *Int. J. Cancer*, 2008, **122**, 664.

S16 S. Watanabe Miyano, Y. Yamamoto, K. Kodama, Y. Miyajima, M. Mikamoto, T. Nakagawa, H. Kuramochi, S. Funasaka, S. Nagao, N. H. Sugi, K. Okamoto, Y. Minoshima, Y. Nakatani, Y. Karoji, I. Ohashi, Y. Yamane, T. Okada, T. Matsushima, J. Matsui, M. Iwata, T. Uenaka, and A. Tsuruoka, *Mol. Cancer Ther.*, 2016, **15**, 2630.

S17 A. Kikuchi, T. Suzuki, T. Nakazawa, M. Iizuka, A. Nakayama, T. Ozawa, M. Kameda, N. Shindoh, T. Terasaka, M. Hirano, and S. Kuromitsu, *Cancer Sci.*, 2016, **108**, 236.

S18 M. Kameda, I. Kuriwaki, K. Iikubo, H. Hisamichi, Y. Kawamoto, H. Moritomo, and T. Suzuki, inventorsNitrogen-containing aromatic heterocyclic compound. 2013 February 26, 2013.

S19 W. Guo, W. H. Hang, and J. S. Li, inventorsNovel pyrimidine and pyridine compounds and their usage. 2014 March 14, 2014.

S20 T. G. Hall, Y. Yu, S. Eathiraj, Y. X. Wang, R. E. Savage, J. M. Lapierre, B. Schwartz, and G. Abbadessa, *PLOS ONE*, 2016, **11**, e0162594.

S21 N. Zhou, Y. Xu, X. Liu, Y. Wang, J. Peng, X. Luo, M. Zheng, K. Chen, and H. Jiang, *Int. J. Mol. Sci.*, 2015, **16**, 13407.

S22 A. Jiang, Q. F. Liu, R. F. Wang, P. Wei, Y. Dai, X. Wang, Y. C. Xu, Y. C. Ma, J. Ai, J. K. Shen, J. Ding, and B. Xiong, *Molecules*, 2018, **23**.

S23 S. Eathiraj, R. Palma, M. Hirschi, E. Volckova, E. Nakuci, J. Castro, C. R. Chen, T. C. K. Chan, D. S. France, and M. A. Ashwell, *J. Biol. Chem.*, 2011, **286**, 20677.